

**S.M. Polyakov**  
**O.S. Polyakov**

## **Introduction into Experimental Gravitonics**

Moscow: "Prometheus" ("Prometey"), 1991

**ISBN 5-7042-0360-4**

## **Introduction into Experimental Gravitonics**

This book is devoted to the issues of producing of gravitation technics and is destined for a wide circle of public (from students to graduated scientists), who are interested in this problem.

The aim of this work is to get the wide circle of creative public to take active part in creation of a new branch of applied scientific researches.

One of peculiarities of this work is a nontraditional view at the problem of Gravitation. This view differs from the traditional one in both basic postulates and methods of approximate working equations derivation. In its essence the work is experimental, since it is begun with "experiments on traditional theory" and finished by "experiments on metal".

In spite of the fact that the developed physical theory agrees with the data of the experiments, the authors do not pretend to know truth. They consider their work to be just a "null approximation" to a future strict theory of Gravitation for which creation there is no enough factual information. However, the approximate equations, which have been derived by the authors, allow make valid laboratory experiments and calculate expected results.

Such devices as sources of gravitation fields, which acceleration of gravity  $g$  is equal to about  $10^{12}$ , sources of non-electromagnetic radiation, which is extended at speed of  $10^{21}$  cm/sec, devices for detecting of this radiation can be reproduced in any laboratory.

Here are the basic results of this work.

The fundamental unit is a physical microstructural model of electron. In spite of it is interesting itself nevertheless the authors use it as a mean to derive the approximate equations, which connect magnetism with gravitation and the gravitation with rotation of material objects.

These equations are primary and allow deduce a set of derived working equations which permit experimental testing.

In this work there are the results of experimenting on classical gravitational-optic effects of General Relativity (GR), i.e. light beam curvature and displacement of optic radiation frequency in a non-homogeneously magnetized ferromagnetic.

The experimental results quite correspond to theoretical forecast.

An analysis of the obtained issues allowed forecast an entirely new, "square", gravitational-optic effect, which consists in the fact that light curvature must be accompanied by displacement of photon frequency. The effect of displacement of optic radiation frequency, which occurs in a non-

homogeneously magnetized ferromagnetic, allow expect displacement of a neutrino flow, which is analogous to the “just gravitational” effect of light beam curvature.

The neutrino flow is connected in a “neutrino trap” which radius of crookedness is about 1 kilometer. Application of such devices in neutrino experiments can  $10^8 - 10^{10}$  times increase their effectiveness.

One of the achievements of our approximate theory is an explanation of magnetostriction as a secondary gravitation effect. Just a magnetization curve of a concrete material is necessary to calculate the whole magnetostriction curve.

In the authors’ opinion, a magnetostriction constant is gravitation energy, which is cumulated by a ferromagnetic in the magnetization saturation point.

The speed of gravitation radiation extension at “recoil” momentum was experimentally calculated. At the experiments the mechanical equations, which connect gravitation with rotation of a material body, were widely tested.

At the same time it was found out that the gravitation radiation is of two types, i.e. “dipole” and “quadrupole”.

Dipole radiation corresponds to the case of non-stationary rotation of an object, which maintains its geometry for the operational cycle. Its speed comes to  $10^8 - 10^9$  C.

The quadrupole radiation is a radiation of a mechanical system, which changes its geometry for the operational cycle. Its speed is strictly defined and comes to  $3 \cdot 10^{10}$  C ( $\pm 30\%$ ) that allows consider this magnitude as “a secondary fundamental constant of matter extension”.

Supposing physical processes to be reversible we obtain a great amount of engineering solutions of the problem of detection of radiation of the new type.

Certainly, many principal difficulties and obstacles of organization are yet to come. However, in the whole, it has been started to solve the problem of gravitational technics creation.

Authors.

## Part 1

# Research for Ways of Solution of the Problem of Powerful Laboratory Sources of Gravitation radiation

## Chapter 1

### New notions of long ago forgotten concepts

This work is written for those people who have a quite superficial notion of General Relativity by A. Einstein but have studied a course of general physics, who are experienced in self-dependent experimental work and desire to work in the centre of the modern science. Let us not waste time to inexpertly criticize General Relativity by A. Einstein and its various modifications, which pretend to be self-dependent. It is enough to remember that nowadays there are neither gravitation spaceships nor communication systems based on gravitation fields. Therefore, let us gain understanding of the subject by ourselves.

We will take a certain succession of well-known scientific concepts, facts and phenomena. In spite of they were found out long ago, on closer examination these facts appear to be imperfectly known.

### § 1. Is the “light barrier” penetrable?

The reply of both GR and SR (Special Relativity) by A. Einstein for this question is strong **NO!** In spite of the possibility of “super-light” particles existence, i.e. tachions, is not refused by the modern science. Adherents of GR and SR ground their objections by the following way: it is known that making motion relatively an unmovable observer the parameters of the physical object are changed in proportion to its speed. The mass increases according to the following equation

$$m_x = \frac{m_0}{\sqrt{1 - \left(\frac{v}{c}\right)^2}} = \frac{m_0}{\Gamma}, \quad (1)$$

and the volume decreases

$$V_x = V_0 \cdot \sqrt{1 - \left(\frac{v}{c}\right)^2} = V_0 \cdot \Gamma, \quad (2)$$

where  $v$  is speed of the body moving relatively the observer,  
 $c$  is the light speed,

the length decreases as well

$$L_x = L_0 \cdot \Gamma. \quad (3)$$

An effective force, which is necessary for mass  $m_0$  acceleration, increases in accordance to the equation of

$$F = \frac{d}{dt}(P) = \frac{d}{dt} \left( \frac{m_0 v}{\sqrt{1 - \left(\frac{v}{c}\right)^2}} \right) = \frac{d}{dt} \left( \frac{m_0 \cdot v}{\Gamma} \right) \quad (4)$$

and becomes infinite at  $v=c$ .

Thus, at  $v=c$  the mass becomes infinite, and the volume  $V$  vanishes. To achieve the speed of  $v=c$  an infinite force is required, i.e. to “penetrate  $c$ -barrier” an infinite mass requires an infinite energy, hence the penetration is impossible. All that sounds so solid and convincing that such a simple question as: whether mass can exist without volume? – is not asked. What will occur if a product of the mass by the volume is accepted as a “characteristic parameter”?

It is evident that Lorentz transforms (1, 2, 3) do not make any influence on this product:

$$m_x \cdot V_x = \frac{m_0}{\Gamma} \cdot V_0 \cdot \Gamma = m_0 \cdot V_0 = \text{invariant.} \quad (5)$$

Lorentz transforms do not influence on the transverse size of the physical object in the case of rectilinear motion; hence the equation (5) may be rewritten as following:

$$m_x \cdot L_x = m_0 \cdot V_0 = \text{inv.} \quad (6)$$

Now let us think if in the nature there are real physical objects which satisfy the equation (6).

Let us analyze an electromagnetic wave. It has equivalent mass of  $m = \frac{h \cdot \nu}{c^2}$  and a characteristic length  $\lambda$ . In accordance to the equation (6):

$$m \cdot \lambda = \text{inv.} \quad (7)$$

However,

$$m \cdot \lambda = \frac{h}{c} \quad (8)$$

is a definition of “Compton wave”, where  $h$  is Plank constant,  $c$  is the light speed, and the quotient of  $\frac{h}{c} = \text{inv}$  is a quotient of two world constants.

Thus our hypothesis (5) has been proved.

Now if the both parts of the expression (8) are multiplied by the frequency of this wave we will derive an equivalence principle of any quantum of electromagnetic radiation:

$$m \cdot \lambda \nu = \frac{h \cdot \nu}{c}, \text{ but } \lambda \nu = c, \text{ hence } mc^2 = h\nu. \quad (9)$$

**Hypothesis. Lorentz transforms are valid for any speed.** Let us try to look over the “light barrier”. Obviously, for penetrability of “c-barrier” for matter in general it is necessary for geometry and mass of a matter to be valid magnitudes at the both sides of the “c-barrier”. That is possible always supposing both the mass and the geometry to be two-component magnitudes, i.e. they both must have a real component and a virtual one, i.e. they must be “dual magnitudes”. For example:

$$\begin{cases} m_1 = m_2 \\ m_2 = +jm_0 \end{cases} \quad \begin{cases} L_1 = L_0 \\ L_2 = -jL_0 \end{cases}, \text{ where } j = \sqrt{-1}. \quad (10)$$

In this case  $m_1L_1 = m_2L_2 = \text{inv.}$

Fig.1  
Relativistic parameters of an object, which has both two-component mass and length.

Relativistic parameters of a physical object, which has both two-component mass and length, are represented in Fig. 1. Since now we have doubts in everything including the absolute value of “barrier speed” then we will use  $c_B$  instead of  $c$  in Lorentz transforms. For the present moment the index of  $c_B$  is accepted as unknown. The curves, which are demonstrated in the graphical chart, show the character of change of complex parameters  $m_x$  and  $L_x$  normalized to one that occurs in the speed interval of  $0 \leq \frac{v}{c_B} \leq 3$ . Real positive values of mass and size are at the both sides of the “c-barrier”.

Hence the object really exists at the both sides of the “c-barrier”.

Thus, if the condition of “c-barrier absolute penetrability” is really fulfilled then “super-light speed flights” are permitted by, at least, Lorentz transforms.

## § 2. Energy proportions and mechanism of “c-barrier” establishing

The classical definition of relativistic kinetic energy is

$$E_k = m_0c^2 \left( \frac{1}{\Gamma} - 1 \right) \quad (11)$$

and at  $\frac{v}{c} \rightarrow 0$  turns into the well-known expression of

$$E_k = \frac{mv^2}{2}. \quad (12)$$

In other cases at  $0 < \frac{v}{c} < 1$ :

$$E_k = \Delta mc^2 = \left( \frac{m_0}{\Gamma} - m_0 \right) c^2. \quad (13)$$

At low speed  $\left( \frac{v}{c} \rightarrow 0 \right)$  the relation between  $E_k$  and the momentum of  $p=mv$  is expressed by the equation:

$$E_k = p \frac{v}{2} = \frac{p^2}{2m}. \quad (14)$$

However, by definition, the relativistic momentum is

$$p = \frac{m_0 v}{\Gamma}. \quad (15)$$

It is not difficult to see that the equation (14) is not totally satisfied at the speed of  $0 < \frac{v}{c} < 1$ :

$$E_k = m_0 c^2 \left( \frac{1}{\Gamma} - 1 \right) \neq \frac{p^2}{2m} = \frac{1}{2} \frac{m_0 v^2}{\Gamma}. \quad (16)$$

The expression of

$$E = \frac{p}{v} \cdot c^2 = \frac{m_0}{\Gamma} \cdot c^2 = m_0 c^2 \left[ 1 + \frac{1}{2} \left( \frac{v}{c} \right)^2 + \frac{3}{8} \left( \frac{v}{c} \right)^4 + \dots \right] = c^2 (m_0 + \Delta m) \quad (17)$$

describes full relativistic energy of the moving object. Thus the accurate one-valid connection between kinetic energy and the momentum of relativistic object that occurs in the interval of  $0 < \frac{v}{c} < 1$  is broken.

It is incomprehensible why nobody has paid attention for this fact.

If the expression is redefined for  $E_k$ , for example, as

$$E_k = \frac{m_0 v^2}{\Gamma} \left( 1 - \frac{\Gamma}{2} \right), \quad (18)$$

then at low speed the equation (18) produces

$$E_k = \frac{m_0 v^2}{1} \left( 1 - \frac{1}{2} \right) = \frac{m_0 v^2}{2} = p \frac{v}{2}$$

without any problem and at high speed ( $v \rightarrow c$ ) it produces

$$E_k = \frac{m_0 v^2}{\Gamma} (1 - 0) = \frac{m_0 v}{\Gamma} \cdot v = p \cdot v, \quad (19)$$

i.e. it ensures a normal transmission of low speed values into relativistic ones. The dependence of  $E_k = f\left(\frac{v}{c}\right)$  of the first definition (11) and the last one (18) is represented in Fig. 2.

$$\text{At the other side of the "c-barrier" } E = \frac{m_0 v^2}{\Gamma} (1)$$

The correction of  $\frac{\Gamma}{2}$  is virtual.

Fig.2

Dependence of the relativistic kinetic energy on speed that is demonstrated for the first definition and for the last one.

It can be seen from Fig. 2 that in the speed interval of  $0 < \frac{v}{c_B} < 1$  the first curve almost coincides with the last one. However significant differences are observed at the other side of the "c-barrier" at  $\frac{v}{c_B} > 1$ .

At  $m = m_0 = +1$  the dependence of  $E_k = m_0 c^2 \left( \frac{1}{\Gamma} - 1 \right)$  (11) is divided into two parts, viz  $E_1 = -m_0 c^2$ , which is the real negative energy, and  $E_2 = -j \frac{m_0 c^2}{\Gamma}$ , which is the virtual negative energy. That real energy seems not to have physical sense, whereas a rational explanation of the virtual energy can be formulated.

It is typical that the dependence of  $E_2 = f\left(\frac{v}{c_B}\right)$  increasing the speed asymptotically tends to zero.

The dependence of  $E_k = \frac{m_0 v^2}{\Gamma} \left( 1 - \frac{\Gamma}{2} \right) = f\left(\frac{v}{c_B}\right)$  at  $\frac{v}{c_B} > 1$  vastly differs from the previous one. For  $m = m_0(1 + j) = 1 + j$  it is divided into 4 curves:

$$\frac{m_0 v^2}{\Gamma}; -j \frac{m_0 v^2}{\Gamma}; -\frac{m_0 v^2}{2}; -j \frac{m_0 v^2}{2}.$$

Nevertheless, since  $\frac{\Gamma}{2}$  at  $\frac{v}{c_B} > 1$  is a virtual correction to the real energy component and a real correction to the virtual component then it can be cast out. In Fig.3 there is represented the dependence of the relativistic momentum of  $p = \frac{m_0 v}{\Gamma} = f\left(\frac{v}{c_B}\right)$  and the energy of  $E = p \cdot v = \frac{m_0 v^2}{\Gamma} = f\left(\frac{v}{c_B}\right)$  that at  $\frac{v}{c_B} < 1$  coincides with neither the first definition of the kinetic energy nor with the last one (however it is numerically similar). However if the virtual correction of  $\frac{\Gamma}{2}$  is removed then at  $\frac{v}{c_B} > 1$  then it precisely coincides with the last definition.

Fig.3

Dependence of  $p$  relativistic momentum and the energy of  $E = pV$  on speed.

Now let us observe the results of “incorrect” formulation of the relativistic energy of a moving material body.

1. At relative (standardized) speed of  $\frac{v}{c_B} \cong 0.85$  the energy of a moving body is equal to one, i.e. it comes to the equivalent energy of rest mass of  $m_0 c^2$ .
2. At the other side of “c-barrier” in the speed interval of  $1.25 \leq \frac{v}{c_B} \leq 1.5$  a “potential hollow” appears. It has minimal energy, which is equal to  $2mc^2$  ( $E_{\min} = 2 \cdot m_0 c^2$ ).
3. In the “pre-light area” the full energy of a moving body is equal to  $2mc^2$  at  $0.85c_B$  speed as well. Here is a natural question occurs: whether it means that the penetration of the “c-barrier” is similar to the “tunnel-effect”? Perhaps, the infinite energy is not required to penetrate the “c-barrier” but the penetration occurs self-dependently as a jump when the speed of  $0.85c_B$  is achieved?

The elementary analysis of the problem of “c-barrier” penetrability, which is stated above, was made by the author in 1975. Nevertheless, first indirect proof of our method relevance appeared 10 years later, when D.D. Ivanenko and his colleagues published their “Calibration Gravics” [1]. In this book there is demonstrated a four-dimensional theory of “scalar gravity field, which has dynamic torsion”, which describes two types of scalar particles, viz a real mass  $M_1$  and a virtual mass  $jM_2$ .

Thus our ten-year-aged reasons are not contrary to the newest concepts of Dynamic Gravics. Unfortunately, a complex character of geometry is not mentioned in this work. It is evident that even this elementary level of the observation of “c-barrier” problem produces numerous questions and hypotheses. Therefore to avoid superfluous discussions we conclude by that has already said above.

In conclusion we beg to note that, according to the principle of equivalence of mass and energy, the value of  $\frac{v}{c_B} \cong 0.85$  (see Fig.2) is a domain of photon existence. Hence the absolute value of “barrier speed” is equal to

$$c_B \cong 1.178c \cong 3.53 \cdot 10^{10} \text{ cm/sec} \quad (20)$$

in our “free space” that can be experimentally tested by direct or indirect ways.

### §3. How much is a photon “electric length”, and how many lengths are contained in one quantum of electromagnetic radiation?

Let us observe V. Geysberg’s indeterminacy principle for both energy of a quantum of electromagnetic radiation and the duration of this quantum, which has been measured by laboratory instruments. The indeterminacy principle for these canonically conjugate multitudes can be written as

$$\Delta E \cdot T \geq h, \quad (21)$$

where  $h$  is Plank constant,

$\Delta E$  is a minimal mistake of energy change, which has physical sense (a mistake, which is proportional to a half of oscillation period, does not have physical sense as it is impossible to measure energy of “a half of a progressive wave”),

$T$  is the length of an envelope curve of the electromagnetic momentum.

Let us observe the minimal value of the expression (21)

$$\Delta E \cdot T = h \quad (22)$$

and replace  $h$  by its value defined from a “constant superfine structure”, i.e.

$$h = 137 \frac{2\pi e^2}{c}.$$

Then the expression (22) turns into

$$\Delta E \cdot T = 137 \frac{2\pi e^2}{c}. \quad (23)$$

Let us make a substitution:  $c = \lambda v = \frac{\lambda}{\tau}$ , where  $\tau$  is a oscillation period of our quantum.

The expression (23) transforms into

$$\Delta E \cdot \frac{T}{\tau} = 137 \frac{2\pi e^2}{\lambda} = \Delta E \cdot N, \quad (24)$$

where  $N = \frac{T}{\tau}$  is a total amount of oscillation periods of a quantum of electromagnetic radiation, i.e. a photon “electric length”. Supposing  $\Delta E = \frac{2\pi e^2}{\lambda}$  to be electromagnetic energy, which is transmitted by the same length of photon wave, we derive

$$N=137. \quad (25)$$

It is evident that the expression (24) is a classical formulation of photon energy:

$$\Delta E \cdot N = \frac{2\pi e^2}{\alpha \cdot \lambda} = \frac{2\pi e^2 hc}{\lambda \cdot e^2} = \frac{hc}{\lambda} = h\nu = E,$$

i.e. the indeterminacy principle, which minimal value is observed, describes the quite certain energy of one photon. Here is a natural question appears: why  $\Delta E = \frac{2\pi e^2}{\lambda}$  is considered instead of  $\Delta E = \frac{e^2}{\lambda}$ ? Then the “electric length” is  $2\pi$  times more. Firstly, it should pay no attention to superficial resemblance of  $\Delta E$  and energy of electrostatic interaction before clarification of photon microstructure. Secondly, this question has already been settled experimentally.

Actually, since  $T = N \cdot \tau = 137 \cdot \tau = \frac{1}{\alpha\nu} = \frac{\lambda}{\alpha c}$  then it is evidently that

$$T = \frac{\lambda}{\alpha c} \quad (26)$$

is the minimal duration of an single photon.

As it is known [2], optic radiation momentum, which is shorter than it is defined by the expression (26), has not been registered by the present.

**Reference:** a) for optic momentum of  $\lambda = 0.63 \cdot 10^{-4}$  cm  $T_{\min} = 0.3 \cdot 10^{-12}$  sec, b) for superhigh frequency momentum of  $\lambda = 3$  cm  $T_{\min} = 1.37 \cdot 10^{-8}$  sec. If, regardless of forecast, a shorter momentum than the expression (26) allows is successfully radiated and measured at  $L$  distance, which greatly exceeds  $137\lambda$ , then this momentum must have some special peculiarities.

#### §4. Is photon a one-massed or two-massed particle?

As it is known, observing wave packet as a superposition of plane transverse waves in quantum radiation theory [3] the equation of harmonic oscillator produces a set of discrete solutions:

$$E_n = h \cdot \nu_0 \left( n + \frac{1}{2} \right), \quad (27)$$

where  $n=0, 1, 2, 3, \dots$  is interpreted as a number of photons, which are connected with this wave. The first solution, where  $n=0$ , describes a “zero photon”, which **electric component and magnetic component are equal to zero**, and **its energy is equal to a half of classical photon energy**.

This energy is unobserved and does not vanish on any condition including the case of absolute zero temperature! Since nowadays the issue of “zero photon” essence remains open and, on our mind, the concept of “vacuum zero oscillations” is uninformative then we presume to declare our point of view on this issue. The photon of  $\frac{hv_0}{2}$  is gravitation energy of a quantum, which in the moment of its generation has come over the “c-barrier” and has been considered to be a virtual magnitude as well as its equivalent mass. In our opinion, just this energy causes such a strange effect as magnetization of a ferromagnetic by a laser beam, which is widely applied in the newest sound recorders and has not yet been provided with a convincing explanation.

Thus a photon has two energies, i.e.

$$E_1 = hv_0 \text{ and } E_2 = -j \frac{hv_0}{2}, \quad (28)$$

and two masses respectively, i.e.

$$m_1 = \frac{hv_0}{c^2} \text{ and } m_2 = -j \frac{hv_0}{2c^2}, \quad (29)$$

where  $m_1$  is the electromagnetic mass,  $m_2$  is the gravitation mass.

Now a natural question appears what the real proportion of the electromagnetic mass and the gravitation mass of a photon is, i.e.

$$\frac{m_1}{m_2} = 2 \text{ or } \frac{m_1}{m_2} = 1? \quad (30)$$

From GR point of view the inertial mass and gravitation mass of any material object are equal! This means that deciding between two proportions of  $E_k = f\left(\frac{v}{c_B}\right)$ , which are represented in Fig.1 and Fig.2, we must choose the “incorrect” one, where the relativistic energy is doubled in the over-barrier “potential hollow”, which is equal to  $2mc^2$ . Hence, the domain of a photon existence corresponds to a photon relative velocity, which is equal to  $0.85c_B$ . Hence the barrier speed absolute value in the free space is

$$c_B \cong 3.53 \cdot 10^{10} \text{ cm/sec.}$$

Now let us suppose that we can control a photon velocity in the free space, i.e. the proportion of  $\frac{v}{c_B}$ , by some unknown means. Then formally we can calculate dependence of photon energy on its relative velocity.

Both this dependence and dependence of the photon frequency on its velocity relatively an unmovable observer are represented in Fig.4, according to the SR known equation of

$$v = v_0 \sqrt{\frac{1 + \left(\frac{v}{c_B}\right)}{1 - \left(\frac{v}{c_B}\right)}}. \quad (31)$$

Fig. 4.

Photon full energy as a velocity function.  $hv_0$  is the photon energy at  $\frac{v}{c_B}$  of 0.850.

Observing these graphical charts in the aggregate it is evident that any change of the photon electromagnetic energy causes a simultaneous change of its frequency. Moreover, the “potential hollow” floor is vertically shifted and a new balance between the electromagnetic component and the gravitation component of the photon energy is reestablished at a new value of frequency  $\nu_x$  as well. In conclusion we note that the elementary statement does not suppose elementary interpretation. We have viewed quite fundamental issues, which the orthodox science provides with evasive answers. Our reasons come to critical points everywhere, i.e. to the possibility of experimental testing.

The questions observed in this chapter are necessary to understand the following material as well as to comprehend the inner logic of the author, who has to look at the world through “gravitational glasses” to see those details, which are invisible in the “electromagnetic light”.

## Chapter 2

### Photon and electron microstructural model

The preliminary work, which has been made in chapter 1, allows us simulate a photon microstructure and then an electron microstructure that is controllable at every step. Why is it necessary? As it is shown in Fig. 5, this is the only way to derive valid working gravity equations, which connect the gravitation with mass rotation as well as with magnetism, i.e. which allow organize valid laboratory experiments.

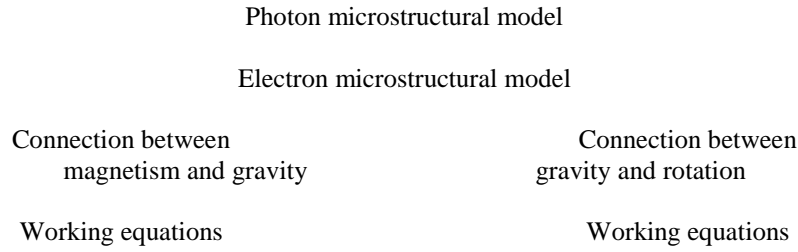


Fig.5  
A scheme of the structure of a “working” theory of gravitation radiation sources.

**§ 1. What do we know of a photon as a quantum of electromagnetic energy?**

1. We know that in the free space the photon phase velocity is equal to a group velocity. Hence, it moves as a rigid construction does until meets an obstacle.
2. A photon has a spin, i.e. an angular momentum, which is equal to such a magnitude as  $\hbar$

$$S_{hv} = \hbar = \frac{h}{2\pi}. \tag{32}$$

3. We have just found out the fact that the photon electric length is equal to  $137\lambda$ , and its energy is super-quantized into 137 parts, which are equal to  $\frac{2\pi e^2}{\lambda}$  each.
4. Moreover, we know that, according to the electrodynamics, all photons are equivalent, i.e. they are described by the same equations independently of a wave length.

There is neither displacement current nor conduction current in the free space. Nevertheless, a photon, as well as its electromagnetic fields and its spin, exists and moves as a rigid construction at C speed in this space. Since that it should be supposed that a photon itself provides the existence of both the fields and the spin. At zero approximation a model of a linear-polarized photon can be represented as an electrostatic construction, which is demonstrated in Fig.6.

Fig.6  
Electrostatic model of a photon (it does not explain its stability of shape).

As it is shown in Fig.6, the model is a system of two linear chains of elementary charges, which are connected by Coulomb force inside of every chain. Moreover, the same Coulomb force connects the different chains. To make it certain, let us accept a distance between any proximal pair of charges as  $\lambda$ . In Fig.6 the arrows demonstrate the direction of forces of electrostatic interrelation between the proximate pairs of charges. In a coordinate system, which moves at C speed, this model can be accepted as static. Since that it is evident that, according to Irnshow theorem [4], this rigid construction of electrostatic charges is impossible to exist.

Moreover, it can be seen from Fig. 6 that every elementary charge, which generates the electromagnetic field of a linear-polarized photon, interacts with four proximate neighbors (i.e. two  $q^+$  and two  $q^-$ ). For the system of 137 pairs as a whole, this interaction causes negative pooled energy of electrostatic interaction of  $\sum Eq = -\frac{e^2}{\lambda}$  at the equal (by convention) distances between any pair of proximate charges. This value comes to just approximately 1/860 part of a photon energy  $h\nu$ , i.e. it is a negligible quantity.

Hence, the nature of photon energy is non-electrical therefore the question of  $2\pi$  multiplier, which is in the subquantum energy definition, is removed. Certainly, we have observed only the zero approximation; however, it is unlikely that the account of the higher levels of electrostatic interaction can fundamentally change the situation. Let us accept our electrostatic model be fundamentally valid but require our subcharges have spins as well. Then it will become full like, for example, in Fig.7. Let us name these elementary subcharges as unquanta and evaluate their parameters.

Fig.7  
Photon complex model (fragment).

## § 2. Uniquantum parameters

### 1. Uniquantum spin (it is postulated)

Since all the unquanta are equivalent and a photon total spin is equal to  $\hbar$  then a spin of one unquantum should be equal to

$$S_u = \frac{\hbar}{2} \cdot \alpha = \frac{1}{137} \cdot \frac{\hbar}{2}. \quad (32a)$$

If all the spins of unlike unquanta, which are included in the photon “construction”, are parallel then the sum of spins of 137 pairs makes the resultant value of a linear-polarized photon spin.

### Photon spin paradox

It is known that a photon spin of any polarization is equal to  $\hbar$ . A photon spin is parallel to spreading direction.

Let us view a photon of  $1\lambda$  length,  $m = \frac{h\nu}{c^2}$  mass and some transversal “radius”  $r$ . The spin equation is as following:

$$S = mr^2 \omega, \quad (33)$$

where  $\omega$  is frequency of photon mass rotation on C axis. At  $\omega = 2\pi\nu$  there is

$$S = \frac{h\nu}{c^2} \cdot r^2 \cdot \omega = \frac{h\nu}{c^2} \cdot \frac{r^2 \omega^2}{\omega} = \frac{h\nu}{\omega} = \hbar, \quad (34)$$

where  $\nu$  is photon proper frequency, and  $\omega r = c$ .

Which photon does describe the equation (34), i.e. linear or circular? If  $\omega = 2\pi\nu$  then the answer is the linear one. Then what is the circular photon spin equal to? What is an elliptically polarized photon spin equal to? I can propose an elementary task for those, who understand everything. It is given 3 photons of  $E = h\nu$  energy. Their energy is equal but of different polarization (i.e. linear, elliptical, and circular). It is to be proved that all three photons have spins  $S = \hbar$ . It must be proved by calculation instead of words. From the point of view of a photon unquantum model there are three possible photon states:

A. *State of Linear Polarization* (Fig.8, a)

A photon spin is equal to the sum of unquanta spins; however it is orthogonal to the spreading direction.

$$S_{\perp} = \sum S_u = \frac{2}{\alpha} \cdot \frac{\hbar\alpha}{2} = \hbar, \quad (35)$$

where 
$$S_u = \frac{\hbar\alpha}{2}, S_{\perp} = \hbar, S_{\parallel} = 0.$$

In both a photon coordinate system (x, y, c) and a laboratory coordinate system

$$S = S_{\perp} + S_{\parallel} = \hbar.$$

a.

b.

c.

Fig.8  
The photon spin, according to the unquantum model.

B. *Non-rotating photon, which is polarized by circle.* (Fig.8, b)

In the photon coordinate system (x, y, c)

$$S_{\perp} = \sum S_u = 0, S_{\parallel} = 0, \text{ as } \omega = 0.$$

In the laboratory coordinate system

$$S_{\perp} = 0, S_{\parallel} = 2m_u r^{2\omega}. \quad (36)$$

$2m_u$  is a mass of a pair of unquanta rotating relatively an unmoving flat, which is orthogonal to the direction of the photon motion.

$2m_u = \frac{\alpha h\nu}{c^2}$ ;  $\omega r = c$ ;  $\omega = 2\pi\nu\alpha$ , i.e. an angular displacement of a pair is  $u - \tilde{u}$  at a way of  $1\lambda\Delta\varphi = \frac{2\pi\alpha}{\lambda}$ . Then for an unmoving observer there are

$$\begin{aligned} S_{\parallel} &= \frac{\alpha h\nu}{c^2} \cdot \frac{\omega^2 \cdot r^2}{\omega} = \frac{\alpha h\nu}{2\pi\nu\alpha} = \hbar; \\ S_{\perp} &= 0; S = S_{\perp} + S_{\parallel} = \hbar. \end{aligned} \quad (37)$$

### C. Rotating photon, which is polarized by circle

In the photon coordinate system there are

$$\begin{aligned} m &= \frac{h\nu}{c^2}; \omega = 2\pi\nu; \omega r = c; \\ S_{\parallel} &= \frac{h\nu}{c^2} \cdot r^2 \cdot \omega = \frac{h\nu}{c^2} \cdot \frac{r^2 \omega^2}{\omega} = \frac{h\nu}{2\pi\nu} = \hbar; \\ S_{\perp} &= 0; S = S_{\perp} + S_{\parallel} = \hbar. \end{aligned} \quad (38)$$

In the laboratory coordinate system there are

$$\begin{aligned} S_{\parallel} &= 2m_u \cdot \omega \cdot r_x^2; \omega = 2\pi\nu; 2m_u = \frac{\alpha h\nu}{c^2}; \\ S_{\parallel} &= \frac{\alpha h\nu}{c^2} \frac{(\omega^2 \cdot r_x^2)}{2\pi\nu} = \alpha \cdot \hbar \cdot \frac{(\omega^2 \cdot r_x^2)}{c^2}; \end{aligned} \quad (39)$$

$$S_{\parallel} = \hbar \text{ only if } r_x = r_0 \sqrt{\alpha}. \quad (40)$$

A fast rotating photon is  $\frac{1}{\sqrt{\alpha}}$  times “compressed” in a transversal direction.

The described A, B, C models allow experimental testing and cause two consequences:

1. A photon spin is defined by two components, which sum is equal to  $\hbar$ :

$$S_{\perp} + S_{\parallel} = \hbar.$$

2. At the equal energy of  $E = h\nu$  the photons of different polarizations must interact with matter in different ways.

## 2. Uniquantum magnetic momentum (it is postulated)

Here we will permit to adapt the data to the result, viz let us suppose a uniuantum magnetic momentum to be equal to 1/3 of difference between an electron magnetic momentum and Bohr magneton, i.e.

$$\mu_u = \pm \frac{1}{3} \frac{\alpha}{2\pi} \mu_b = \pm \frac{\alpha}{6\pi} \mu_B. \quad (41)$$

This assumption will produce an unexpected effect at electron modeling.

## 3. Uniquantum gravitation mass (it is postulated)

The uniuantum gravitation mass is defined by the equivalent mass of zero photon:

$$m_u = \frac{h\nu}{2} \cdot \frac{\alpha}{2c^2}. \quad (42)$$

An actual value of this mass for our sub-light space is

$$m_u = -j \frac{h\nu}{2} \frac{\alpha}{c^2}, \quad (43)$$

i.e. virtual value, which is doubled in the “potential hollow”, i.e.  $2mc^2$ .

## 4. Equivalent charge and radius of uniuantum

We consider the uniuanta as magnetostatic particles, which do not have electric field in an unmovable coordinate system. However, according to electrodynamics laws, consisting of a photon the proper static magnetic field of every uniuantum will generate an alternating electric field in the laboratory coordinate system. In this case an electric field, which is related to one uniuantum, is equivalent to some electrostatic charge appearance, which we can approximately evaluate. Nevertheless, it should be remembered the fact that actually a uniuantum does not have a charge.

It follows the magnetic momentum definition that

$$\begin{aligned} \mu_u &= \frac{q_u r_u}{2} = \frac{\alpha}{6\pi} \mu_B; \\ q_u &= \frac{\alpha}{3\pi} \frac{\mu_B}{r_u} = \frac{\alpha}{3\pi} \cdot \frac{e_0 r_0}{2\alpha \cdot r_u} = \frac{e_0}{6\pi} \cdot \frac{r_0}{r_u}, \end{aligned} \quad (44)$$

where  $r_0$  is an electron radius,  $e_0$  is an electron charge.

Let us suppose  $q_u = e_0$  at  $E=0.511$  Mew. Then

$$q_u = e_0 \left( \frac{1}{6\pi} \cdot \frac{r_0}{r_u} \right) = e_0 \cdot 1$$

or

$$r_u = \frac{r_0}{6\pi}.$$

However, an electron radius is in accord with the proportion of

$$\frac{2\pi r_0}{\alpha} = \lambda_c, \quad (45)$$

where  $\lambda_c$  is Compton wave length,

or

$$r_0 = \frac{\alpha \lambda_c}{2\pi}.$$

Making a substitution in (44) we derive:

$$r_u = \frac{\alpha \lambda_c}{12\pi^2} \quad (46) \text{ for } 0.511 \text{ Mew}$$

$$r_u = \frac{\alpha \lambda}{12\pi^2} \quad (47) \text{ for any energy}$$

$$r_u \cong 6.18 \cdot 10^{-5} \cdot \lambda.$$

Now we can write the definitive expression for the uniaquantum equivalent charge:

$$q_u = \frac{\alpha}{3\pi} \cdot \frac{\mu_B}{r_u} = \frac{\alpha}{3\pi} \frac{\mu_B \cdot 12\pi^2}{\alpha \lambda} = \frac{4\pi}{\lambda} \mu_B;$$

$$q_u = \frac{4\pi}{\lambda} \mu_B. \quad (48)$$

Another expression can be derived for  $q_u$ :

$$q_u = \frac{e_0}{6\pi} \cdot \frac{r_0}{r_u} = \frac{e_0}{6\pi} \frac{\alpha \lambda_c}{2\pi} \cdot \frac{12\pi^2}{\alpha \lambda} = e_0 \frac{\lambda_c}{\lambda}, \quad (49)$$

which is equivalent to the equation (48).

## 5. Uniaquantum tangential rotation speed

Since we postulate the existence of new super-elementary particles, which pretend to be “prior matter”, then we must describe their properties in every detail. A tangential speed  $v_u$  is an important parameter

as the product of  $\omega \cdot r = c$  is practically always valid in quantum calculations. What is the expression of  $\omega_u \cdot r_u = v_u$  equal to? Let us apply the spin definition:

$$S_u = m_u \cdot v_u \cdot r_u = \frac{\hbar}{2} \cdot \alpha .$$

It follows from this:

$$v_u = \frac{S_u}{m_u \cdot r_u} . \quad (50)$$

Supposing the unquantum radius defined by the expression (47) to be the equivalent of  $r_u$  radius in the equation (50) we will derive

$$v_u = \frac{\alpha \cdot h}{4\pi} \cdot \frac{4c^2}{hv\alpha} \cdot \frac{12\pi^2}{\alpha\lambda} = \frac{12\pi c}{\alpha} = const ; \quad (51)$$

$$v_u = 137 \cdot 12\pi \cdot c = 5.16 \cdot 10^3 c .$$

## 6. Unquantum magnetic field

We have already known that a unquantum has a magnetic momentum and a spin. Moreover, if it is included in a photon then it obtains some equivalent charge. Assuming a unquantum electromagnetic energy to have only magnetostatic origin we can write:

$$E_u = \frac{hv\alpha}{2} = \mu_u \cdot H_u , \quad (52)$$

where  $H_u$  is a unquantum proper magnetic field, which origin is unknown.

From the equation (52) we derive:

$$H_u = \frac{hv\alpha}{2\mu_u} = \frac{hv\alpha}{\frac{\alpha}{6\pi} \cdot \mu_B} = \frac{6\pi hv}{\mu_B} . \quad (53)$$

For the photons, which have the energy of 0.511 Mew, there is

$$H_u \cong 1.68 \cdot 10^{15} \text{ Oersted} . \quad (54)$$

## 7. Unquantum gravitation constant

Since nowadays the radius  $r_u$  is a natural limit of our interest, and, by definition, the unquantum has its proper gravitation energy and gravitation field then let us accept its radius to be equal to the gravitation radius. Then the gravitation constant  $\gamma_u$  becomes:

$$\gamma_u = \frac{r_u \cdot c^2}{m_u} = \frac{\alpha \lambda}{12\pi^2} \cdot \frac{4c^4}{h\nu\alpha} = \frac{\lambda^2 \cdot c^2}{3\pi^2 h} \quad (55)$$

and for the photon of 0.511 Mew energy there is

$$\gamma_u \cong 9.3 \cdot 10^{+36} \text{ cm}^3 / \text{g} \cdot \text{c}^2. \quad (56)$$

In contrast to the other parameters,  $\gamma_u$  increases as the wave length increases.

## 8. Uniquantum gravitation field

On the surface of a radius of any Schwarzschild sphere a scalar gravitation potential (i.e. gravitation field) is equal to  $c^2$ :

$$\varphi_u = \gamma_u \frac{m_u}{r_u} = c^2 = 9 \cdot 10^{20} \text{ cm}^2 / \text{sec}^2, \quad (57)$$

where  $\varphi_u = \text{const}$  and is independent of the uniuantum energy.

Hence, we have calculated (although rather approximately) the parameters of that “prior matter”, which is traditionally called as “Dirack electron-positron sea”. To make it clear this information is represented in Table 1. In future it will be known if the table is valid or not. Nevertheless, it does not have analogues or prototypes (first it was calculated by the author in 1975).

Table 1

### Uniquantum basic parameters

№	Parameter	Defininition	Numeral value for $h\nu = 0.511 \text{ Mew}$	Comment
1.	Spin	$S_u = \frac{\alpha \hbar}{2} = \frac{\hbar}{2} \cdot \frac{1}{137}$	const	Postulated
2.	Magnetic momentum	$\mu = \pm \frac{\alpha}{6\pi} \mu_B$	const	Postulated
3.	Gravitation mass	$m_u = \frac{h\nu\alpha}{4c^2}$	$\approx 1.66 \cdot 10^{-30} \text{ g}$	Postulated
4.	Gravitation radius	$r_u = \frac{\alpha \lambda}{12\pi^2}$	$r_u = \frac{r_0}{6\pi}$	$r_0 = 2.8 \cdot 10^{-18}$ classical electron radius
5.	Equivalent charge	$q_u = \frac{4\pi}{\lambda} \mu_B = e_0 \frac{\lambda_c}{\lambda}$	$q_u = e_0^-$	Exists consisting of a photon
6.	Tangential rotation speed	$v_u = \frac{12\pi}{\alpha} \cdot c$	const	$v_u \cong 5 \cdot 10^3 \text{ C}$
7.	Magnetic field	$H_u = \frac{6\pi h\nu}{\mu_B}$	$1.68 \cdot 10^{+15} \text{ e}$	

8.	Gravitation constant	$\gamma_u = \frac{\lambda^2 c^2}{3\pi^2 h}$	$\approx 9.3 \cdot 10^{+36} \frac{cm^3}{g \cdot c^2}$	
9.	Gravitation field	$\varphi_u = c^2$	const	By definition

As it can be seen from the table, space rigidity of a form of uniuquanta collective, which produce a photon, is determined by a system of fields. They are electrostatic field, magnetostatic field, and gravitation field, which act simultaneously. The parameters of the fields are approximately known. In this case a subquantum energy, which is numerically equal to  $\frac{2\pi e^2}{\lambda}$ , is clear as it represents the action of the whole system of different physical fields.

Now since we know parameters of the subelementary particles and can apply the already known information about the photon then we can try to derive its space structural model.

### § 3. Photon model

A photon model, which has real fields spreading, is represented in Fig.9. Here the following indexes are accepted:

$u$  is the uniuquantum ( $H_u$  and  $\mu_u$  are antiparallel to the spin  $S_u$ ),

$\tilde{u}$  is the antiuniquantum ( $H_{\tilde{u}}$  and  $\mu_{\tilde{u}}$  are parallel to the spin  $S_u$ ).

Arrows show the spreading of a transversal component of the magnetic field of  $H_u$ . It is evident that the sum of the spins is equal to  $\hbar$ , and the sum of all the energies is equal to  $\frac{3}{2}h\nu$ , where the electromagnetic energy of  $h\nu$  ensures the photon interaction with the outer world, and the gravitation one of  $\frac{h\nu}{2}$  ensures the stability of photon shape during this interaction. There is no any vacuum zero oscillations!

Validity of the produced photon model is easy to be experimentally tested.

1. When a plane electromagnetic wave goes through a diffracting lattice the going maximum is at the magnetic vector  $H$  orientation parallel a gap. First this effect was observed by G.S. Gorelik [5] in 50-s during the investigation of plane electromagnetic waves of centimeter diapason. In this case there are the uniuquanta, which have spins. Since that rounding the gap it is not necessary to twist rotation axis of a microgyroscope at this photon orientation relatively the gap. Probably, that may require more energy consumption (therefore the photon does not "move").
2. The minimal duration of a single quantum of any homogeneous electromagnetic radiation in the free space can not be shorter than

$$T = \frac{\lambda}{\alpha \cdot c} = \frac{137 \cdot \lambda}{c}$$

(on condition that during measuring the distance between a generator and a receiver greatly exceeds 137 wave lengths). If some shorter moments are registered in the free space then they should have some physical peculiarities.

Fig.9

Photon space model, which is in X, Y, C coordinate system. The electrostatic charge and the field are absent.

3. According to our model (Fig.9), a linear-polarized photon must magnetize a ferromagnetic, when the electrical vector  $\vec{E}$  is orthogonal to the ferromagnetic flat. In this case the photon leaves a unipolar-magnetized trace. (Fig.10)

**Reference:** One quantum magnetic field for a photon, which has the energy of 2 eV, comes to approximately  $6 \cdot 10^9$  Oersted.

4. The photon electrostatic model (see Fig.6) produces an uncompensated excess of Coulomb interaction energy of  $\frac{e^2}{\lambda}$  range. Hence, the photon must have the trace of the uncompensated charge. If this is the case then the geometrical optics laws must be broken at the repulsion of the photon of an electrically charged surface.

Fig.10

Effect of “optic magnetization” (control of the photon model).

#### § 4. Electron phenomenological microstructural model

$2\gamma$  annihilation of the pair ( $e^+ - e^-$ ) causes generation of two photons, each of which has 0.511 Mew energy. These photons equivalent mass is exactly corresponding to the mass of the initial particles (i.e. electron, positron), i.e. is equal to  $9.1 \cdot 10^{-28}$  g. That we accept as a basis of our reasoning. Hence, we can suppose an electron, a positron and a photon (which energy is equal to 0.511 Mew) to be three different states of the same physical object. We have already decoded the photon structure, now we need find out consistent conditions of a photon transformation into an electron (positron). Let us revise our knowledge of a rest electron.

1. It has an electric charge of  $e_0^- = -4.8 \cdot 10^{-10}$  SGSE units =  $-1.602 \cdot 10^{-19}$  k.
2. It has a rest mass of  $m_0 \cong 9.1 \cdot 10^{-28}$  g.
3. It has a magnetic momentum of  $\mu_0 = \mu_B (1 + \frac{\alpha}{2\pi})$  erg/Gs.
4. It has a spin of  $S_0 = \frac{\hbar}{2} = 0.527 \cdot 10^{-27}$  erg. sec

5. It has an electron classical radius of  $r_0 \cong 2.8 \cdot 10^{-18}$  cm.
6. It has a wave length of the electronic photon of  $\lambda_0 \cong 2.426 \cdot 10^{-10}$  cm.

At first let us pay attention to the fact that even one wave length of an electronic photon can not be placed on the circle of the classical radius. Nevertheless, it is well known that the electron has wave properties.

The perimeter of the circle of the classical radius of the electron is equal to

$$L_0 = 2\pi r_0 = 1.755 \cdot 10^{-12} \text{ cm.} \quad (58)$$

To place at least one wave length of the photon, which has 0.511 Mew energy, on the circle of the classical radius it is necessary virtually to compress the photon

$$\frac{\lambda_0}{L_0} = \frac{2.426 \cdot 10^{-10} \text{ cm}}{1.755 \cdot 10^{-12} \text{ cm}} \cong 137 \text{ times.} \quad (59)$$

According to invariance relation (see chapter 1, §1), we can derive the expression of

$$m_1 \cdot L_0 = m_0 \cdot \lambda_0 = inv, \quad (60)$$

hence

$$m_1 = m_0 \frac{\lambda_0}{L_0} = 137 m_0. \quad (61)$$

To find out the physical sense of the mass  $m_1$  let us produce the product of three magnitudes, i.e.

$m_1 \cdot c \cdot \frac{r_0}{2}$ . Let us substitute the indexes with their numeral values and calculate the result:

$$m_1 \cdot c \cdot \frac{r_0}{2} = 0.527 \cdot 10^{-27} \text{ erg} \cdot \text{sec} = \frac{\hbar}{2} = S_0. \quad (62)$$

We have derived the numerical value of the electron spin as the mechanical momentum that even now is considered by some outstanding scientists to be impossible. Surely, in 1975, when this result was first obtained, experts did not accept it.

Now let us try to explain this result. Let us assume that, as well as in the case of the “zero photon” of  $\frac{h\nu}{2}$ , the mass  $m_1$  is located “over the c-barrier”, where it is a virtual magnitude. The parameter of  $\frac{r_0}{2} = r$  is a physical limit of the mass  $m_1$ , which is located “over the c-barrier”, therefore it is natural to accept the parameter to be equal to an electron gravitation radius.

Then the product of  $m_1 \cdot c \cdot r_1$  completely corresponds to the electronic spin interpretation. Now as we have known the gravitation radius of  $r_1 = \frac{r_0}{2}$  and the electron gravitation mass of ( $m_1 = 137 \cdot m_0$ ) we can derive a gravitation constant of strong interaction of a rest electron:

$$\gamma_e = \frac{r_0}{2} \frac{c^2}{m_1} = \frac{r \cdot c^2 \alpha}{2m_0} = \frac{2.8 \cdot 10^{-13} \cdot 9 \cdot 10^{20}}{2 \cdot 9.1 \cdot 10^{-28} \cdot 137} \cong 1.01 \cdot 10^{+33} \text{ cm}^3 / \text{g} \cdot \text{sec}^2. \quad (63)$$

And after this we can compute the electron gravitation energy:

$$W_e = -\gamma_e \frac{2m_1^2}{r_0} \cong 1 \cdot 10^{+33} \frac{2(137 \cdot 9.1 \cdot 10^{-28})^2}{2.8 \cdot 10^{-13}} \cong 1.11 \cdot 10^{-4} \text{ erg}. \quad (64)$$

Let us evaluate the proportion of the gravitation component and the electromagnetic component of the electron energy:

$$\frac{W_e}{E} = \frac{1.11 \cdot 10^{-4}}{8.9 \cdot 10^{-7}} \cong 137 = \frac{1}{\alpha} = \frac{m_1}{m_0}. \quad (65)$$

It is a very interesting coincidence of  $\frac{W_e}{E} = \frac{m_1}{m_0}$  if we pay attention to

$$W_e = -\gamma_e \frac{m_1^2}{r_1} = -\gamma_e \frac{m_0^2 \cdot 2}{\alpha^2 \cdot r_0}, \text{ and } E = m_0 c^2.$$

However, let us return to the invariance relation (60) Taking into account that the mass  $m_1$  is an over-barrier multitude of

$$m_1 = -j \frac{m_0}{\alpha} \quad (66)$$

we come to a paradoxical conclusion that there is no any electromagnetic wave, which has physical sense, on the electron orbit of the classical radius. It follows the fact that, according to the proportion (43), only a virtual wave length of the type of

$$\lambda_1 = L = j\alpha\lambda_0 \quad (67)$$

is possible for the mass  $m_1$ , else the proportion (60) can not be valid. What does the corpuscular-wave dualism of the electron mean in this case? Let us view Bohr magneton definition to answer this question:

$$\mu_B = \frac{\hbar}{2} \frac{e_0}{m_0 c} = \frac{m_0 c \cdot r_0}{2\alpha} \frac{e_0}{m_0 c} = \frac{m_0}{\alpha} \frac{r_0}{2} \cdot \frac{e_0}{m_0}. \quad (68)$$

Hence, we have found out that Bohr magneton is defined by the product of the gravitation mass, the gravitation radius and the proportion of the charge to the electron mass. After all reductions the expression looks like

$$\mu_B = \frac{r_0 e_0}{2\alpha}. \quad (69)$$

Nevertheless, the real value of the electron magnetic momentum insignificantly differs from Bohr magneton value, i.e.

$$\mu_0 = \mu_B \left( 1 + \frac{\alpha}{2\pi} \right) = 1.00116 \mu_B = \mu_B \left( 1 + \frac{3\alpha}{6\pi} \right). \quad (70)$$

Now let us remember that in one's time we defined a uniuantum magnetic momentum as

$$\mu_u = \pm \frac{\alpha}{6\pi} \mu_B. \quad (71)$$

Then the expression (70) can be rewritten as

$$\mu_0 = \mu_B \pm 3\mu_u. \quad (72)$$

This is the answer for the question of what is on the electron orbit of the classical radius. There are just three uniuanta! Every uniuantum has a charge of  $q_u = e_0^-$ , a magnetic momentum of  $\mu_u = \frac{\alpha}{6\pi} \mu_B$ , a virtual mass of  $m_u = -j \frac{\alpha}{2} \frac{h\nu}{c^2}$ , a proper magnetic field of  $H_u \cong 1.68 \cdot 10^{15}$  E, and a proper spin of  $S_u = \frac{\alpha \hbar}{2}$ . Naturally, the listed parameters are not enough to explain the mass of rest therefore the electron equivalent energy, which is equal to 0.511 Mew, is not enough as well. In practice it is needed the electron magnetostatic energy, which is defined by the product of the proper magnetic momentum and the proper magnetic field of the electron. Let us suppose three mentioned uniuanta to go around the electron orbit of the classical radius at  $c$  speed. (Here an electron planetary model has appeared). Then we can formally evaluate the electron magnetic field by the equation of

$$H_e = \frac{m_0 c^2}{\mu_e} = \frac{8.19 \cdot 10^{-7}}{0.92 \cdot 10^{-20}} = 8.9 \cdot 10^{13} \text{ E}. \quad (73)$$

However, there are still three uniuanta on the electron orbit, each of which has a charge equal to the electron charge. Let us return to the definition of Bohr magneton:

$$\mu_B = \frac{e_0 r_0}{2\alpha} = \frac{3e_0 \cdot r_0}{2 \cdot 3\alpha} = \frac{3e_0 \cdot r_0}{2 \cdot 3/137} = \frac{3e_0}{2} \cdot 45.7 \cdot r_0. \quad (74)$$

45.7 value is nothing but a coefficient of the electron space compress, which occurs in the proper powerful gravitation field. In other words, there is

$$r_o = r_x \cdot \Gamma = r_x \sqrt{1 - \left( \frac{v}{c_B} \right)^2}, \quad (75)$$

hence the real size, which is standardized to the free space, is equal to

$$r_x = \frac{r_0}{\Gamma} = 45.7 \cdot r_0. \quad (76)$$

It is the very coefficient to be used in the equation (68), i.e.

$$\mu_B = \frac{3e_0 r_x}{2} = \frac{q \cdot r_x}{2}. \quad (77)$$

That totally corresponds to the classical definition of the magnetic momentum of ring current:

$$\bar{\mu} = \frac{\pi \cdot r_x \cdot i}{c} = \frac{\pi \cdot r_x^2}{c} \frac{e_x \omega}{2\pi} = \frac{r_x \cdot e_x}{2}, \quad (78)$$

where  $r_x$  is the ring radius;

$\omega$  is  $e_x$  charge rotation frequency;

$c$  is the light speed,  $\omega \cdot r_x = c$ .

What does the term of “space compress” mean? Let us remind that in the free space we have defined the domain of the photon existence in the scale of Lorenz transforms velocities as a velocity, which is equal to  $0.85 c_B$ . Now this domain of existence has moved to  $0.9997605 c_B$  point. It is not due to the photon velocity increase but due to the barrier value of velocity decrease. At the same time the photon constant velocity is equal to  $3 \cdot 10^{10}$  cm/sec.

Hence, the value of “c-barrier” depends on the gravitation field instead of the very photon velocity, the barrier velocity value decreases as well as the field increases. (Is it a key for “c-barrier”?) The very photon is a special object, and its velocity in the free space is a world constant.

To test the validity of these reasons let us evaluate the value of the electron proper magnetic field as a ring current field of three unquanta, which are located on the orbit of the classical radius. The radius is 45.7 times compressed. By definition

$$H = \frac{q_x \cdot c}{r_x^2} = \frac{3e_0 \cdot c}{r_0^2} \cdot \Gamma^2 = \frac{3 \cdot 1.6 \cdot 10^{-19} \cdot 3 \cdot 10^{10}}{(2.8)^2 \cdot 10^{-25} (45.7)^2} = 8.9 \cdot 10^{13} \text{ e}. \quad (79)$$

It is a known number, isn't it? Let us compare it with the evaluation (73). Here is

$$q = 3e_0; r_x = \frac{r_0}{\Gamma}.$$

This is not a casual coincidence. We have adopted  $r_x$ , which is included into the numerator of the first power in the equation (74), to the required result. Nevertheless, in the equation (79)  $r_x$  is included into the squared denominator, and the numerical value of the magnetic field of the electron charges ring current coincides with the value, which has been derived due to energy reasons.

Now the electron model is strictly deduced, i.e. practically we can not vary our reasoning any way. Let us clarify the process of a photon transformation into an electron.

a, b, c

Fig.11

Successive steps of a photon “rolling up”

The successive phases of this transformation is represented in Fig.11, a, b, c. Fig.11, *a* demonstrates a photon, which follows a curved trajectory in a curved space (for example, in the gravitation field of the other photon). If the curvature radius of the trajectory achieves that critical value, at which the photon “head” approaches the photon “end”, then the photon self-acquisition occurs that is shown in Fig.11, *b*. In this case the photon absorbs itself leaving just three unquanta on its outer orbit and three unquanta on its inner orbit that is demonstrated in Fig.11, *c*. From the point of view of power engineering, in the “potential hollow of  $2mc^2$ ”, which is located over the “C-barrier”, the energy of  $3h\nu$  value is accumulated. This energy has turned into gravitational one. The energy of  $\frac{3}{137}h\nu$  is left in the “pre-light” space.

Thus the proportion between the gravitational matter and the electromagnetic matter of the electron has already been established. Now the powerful gravitation field of the already created electron produces an unrepeatable “double C-barrier”, which isolates the inner pre-light space of the outer pre-light space. This case is clearly demonstrated in Fig. 12.

Electrostatic field and magnetostatic field of unquanta

2c-barrier

Fig.12

Allocation of unquanta in the “outer” area and the “inner” area of an electron.

Now to make a valid conclusion it is necessary to accept that the electromagnetic fields of proximate pairs, i.e. unquantum – antiunquantum, which are isolated by the 2C-barrier, are partially closed through the 2c-barrier. As a result the actual value of the electrostatic field of the smeared charge of three unquanta is equal to the field of one electron charge (2/3 of the charge is short-circuited). The proper magnetic fields of the pairs of unquantum – antiunquantum are almost completely closed through the 2C-barrier. The rest of the inner unquanta magnetic field is compensated by the magnetic field of their ring current in such a way that the magnetostatic energy of the electron inner area becomes zero. Hence, the charge is equal to zero in the centre of an electron! The ring current of the outer unquanta ensures the actual value of both the electron magnetic field and the electron magnetic momentum; therefore it ensures its rest mass. The final variant of the electron microstructural model is represented in Fig.13. It is evident that if the photon is turned to the right relatively its world line then an electron is obtained else, i.e. if the photon is turned to the left, a positron is obtained. Depending on the initial orientation of the photon spin for every particular particle summing or subtraction of all magnetic moments and spins (of an electron and its outer unquanta) occur.

In other words, from the point of view of the model, the creation of electrons and positrons of two types is equiprobable. These types correspond to the resultant values of the magnetic momentum and the spin:

$$S_e = \frac{\hbar}{2} \pm 3\alpha \cdot \frac{\hbar}{2} = \frac{\hbar}{2} (1 \pm 3\alpha) = \begin{Bmatrix} 1.0438 \\ 0.9562 \end{Bmatrix} \frac{\hbar}{2} \quad (80)$$

$$\mu_e = \mu_B \left( 1 \pm \frac{\alpha}{2\pi} \right) = \begin{Bmatrix} 1.00116 \\ 0.99884 \end{Bmatrix} \cdot \mu_B. \quad (81)$$

Let us form an expression of

$$g = 2 \frac{\mu_e}{S_e} = \begin{Bmatrix} 1.912 \\ 2.09 \end{Bmatrix}. \quad (82)$$

Fig.13  
Electron three-dimensional microstructural model

The last result is well-known in the theory and the practice of ferromagnetic resonance at SHF as Lande factor or the factor of spectroscopic splitting, which origin is always mysterious. It turns out that Lande factor value is defined by the conditions of an electron creation, and, probably, it may be a controllable magnitude.

The parameters of the electron are demonstrated in Table 2. It follows from the table that the amount of our notions of this issue has significantly increased. Some scientists consider the modeling to be the figment of the imagination, which is devoid of practical value. Let us demonstrate by a simple example that this is not the case. From the standpoint of model notions, the idea of gravitons spontaneous generation, which energy is equal to about 0.5 Mew, at the annihilation of the electron – positron pair does not raise doubts.

This has yet not been observed as there is no appropriate measuring equipment, and this question has not appeared.

It can be said that an annihilation  $\gamma$ -laser is a GRASER at the same time. However, it is not the main result of this model. The main result is the fact that the model shows the simplest way to solve the three basic problems of gravitational technics, which have been discussed above. The simplest way is not always the easiest one; however, it exists and its great part has been already passed. The whole following material is a direct consequent from this electron model.

Table 2

№	Parameter	Definition	Numerical value	Comment
1	Inertial mass	$m_0 = \frac{\mu_e H_e}{c^2}$	$9.1 \cdot 10^{-23} g$	The equivalent mass of the electron magnetostatic energy

2	Gravitation mass	$m_1 = (-j) \frac{m_0}{\alpha}$	$-j \cdot 1.25 \cdot 10^{-25} g$	“over-barrier” mass
3	Classical radius	$r_0 = \frac{e_0^2}{m_0 c^2}$	$2.8 \cdot 10^{-18} cm$	According to an “outer” observer
4	Gravitation radius	$r_\Gamma = \frac{r_0}{2}$	$1.4 \cdot 10^{-13} cm$	According to an “outer” observer
5	Effective radius	$r_e = \frac{r_0}{\sqrt{1 - \left(\frac{v}{c_B}\right)^2}}$	$1.28 \cdot 10^{-11} cm$	According to an “inner” observer
6	“Compress” coefficient of the electron	$X = \frac{1}{\sqrt{1 - \left(\frac{v}{c_B}\right)^2}}$	45.7	————
7	Spin	$S_e = \frac{\hbar}{2} (1 \pm 3\alpha)$	$1.0438 \frac{\hbar}{2}$	<b>Consequence:</b> 2 electron types, 2 positron types
8	Magnetic momentum	$\mu_e = \mu_B \left(1 \pm \frac{\alpha}{2\pi}\right)$	1.00116 0.9984	Analogically
9	Classical charge	$e_0$	$1.602 \cdot 10^{-19} K$	According to laboratory measuring
10	Effective charge	$e_e = 3e_0$	$4.806 \cdot 10^{-19} K$	According to the value of the proper magnetic field
11	Magnetic field	$H_e = \frac{e_e \cdot c}{r_e^2}$	$8.9 \cdot 10^{+13} oersted$	
12	Gravitation constant	$\gamma_e = \frac{r_0}{2} \frac{c^2 \alpha}{m_0}$	$10^{+33} cm^3 / g \cdot sec^2$	
13	Gravitation energy	$W = -\gamma_e \frac{2m_1^2}{r_0}$	$1.11 \cdot 10^{-4} Erg.$	
14	Relation of the electromagnetic energy to the gravitation energy	$\frac{E}{W} = \alpha$	$\frac{1}{137}$	According to “Einstein school of thoughts” $E/W = 3$

## §5. Derivation of approximate gravitational equations, which have practical value

In the strict sense it can not be called as “derivation” since we rather calculate our equations testing and retesting the connections between well-known experimental data and scientific concepts. A wide superficial experimental testing of our equations has been made and successfully resulted. However some problems emerge when very obvious and simple things appear to be far not obvious and simple. In such moments we realize that our approach is very approximate. Nevertheless, we have not known another way by now. Thus, what is the rotating electron gravitational model needed for? The answer is contained in the very question, i.e. the model shows the regularity of the connection of the gravitation with the magnetism and the regularity of the connection of the gravitation with the rotation. The

connection of the magnetism with the rotation was ascertained in the beginning of XX century in the famous experiment, which is known as Einstein-de Haas effect.

Thus the electron is almost exhausted as a source of “fundamental information”, at least, on the level of today notions.

Now let us turn to concrete issues.

a) Connection of magnetism with gravitation

In the previous part (§ 4) we have demonstrated that the relation of the electron electromagnetic energy to its gravitation energy is equal to a hyperfine structure constant, i.e.

$$\frac{E}{W} = \alpha = \frac{1}{137}.$$

In the same part it has been shown that the electron electromagnetic rest mass really has very magnetostatic origin and is determined by the product of the electron magnetic momentum by its proper magnetic field

$$m_0 = \frac{E}{c^2} = \frac{\mu_e H_e}{c^2}. \quad (83)$$

Comparing the equations (83) and (65) we can write:

$$W_e = \frac{\mu_e H_e}{\alpha}. \quad (84)$$

In this case the validity of the equation (84) does not raise any doubts. Now let us turn from the microworld of the electron to the macroworld of a magnetized ferromagnetic. We know that the ferromagnetic state of a matter is generated by the electrons of exchange interaction. We will not penetrate into details of the mechanism of summing of these magnetic moments and the magnetic fields of these electrons (in spite of it may be very important and interesting). We will just revise that the density of the energy, which is supplied by the magnetized ferromagnetic, is defined by the expression of

$$\frac{E_M}{V} = \bar{B} \cdot \bar{H}, \quad (85)$$

where  $\bar{B}$  is an inductance, and  $\bar{H}$  is a proper magnetic field.

Since, by definition, the inductance is a magnetic momentum of a volume unit then the full magnetic energy, which has been supplied in the volume  $V$  of a given ferromagnetic, is equal to

$$E_M = \bar{B} \cdot \bar{H} \cdot V. \quad (86)$$

Supposing the superposition of the magnetic and gravitation fields of particular electrons of exchange interaction to occur according to the same laws (even if the laws are unknown) we can rewrite the equation (84), which concerned a particular electron, for a magnetized ferromagnetic as

$$W = \frac{\overline{BHV}}{\alpha}. \quad (87)$$

The equation (87) demonstrates the common hypothesis of the connection between the magnetic and gravitation fields is erroneous. **The real connection exists between the magnetic and gravitation energy and is realized by matter.** The equation (87) is easy to be experimentally tested in laboratory conditions.

b) Connection of gravitation with rotation

Modeling the electron we have calculated the gravitation constant of strong interaction:

$$\gamma_e = \frac{r_0}{2} \frac{c^2 \alpha}{m_0} \cong 10^{+33} \text{ cm}^3 / \text{g} \cdot \text{sec}^2. \quad (88)$$

At once two questions arise: 1. Why is the gravitation constant of strong interaction?  
2. What will the mechanics obtain from this fact?

As it is known, the Earth gravitation constant is equal to about  $6.67 \cdot 10^{-8} \text{ cm}^3 / \text{g} \cdot \text{sec}^2$  and considered to be a world constant.

Thus we have two world constants, which approximately  $10^{40}$  times differ from each other. There are too many of world gravitation constants. Now we are combining two interactions, i.e. strong interaction and gravitational interaction. At the beginning let us ask a question: what features are common for both the Earth and the electron? The answer is following:

Both the objects have a rest mass, a spin, a proper magnetic field, and a proper gravitation field.

Hypothesis: “Only a rotating object has its proper gravitation field”. An unmoved object, which is located in gravitation field of an outer source, has just a gravitation polarization. At the interactions it behaves just as a field source, like Armko iron swarf does in the field of a permanent magnet.

One more hypothesis: “A gravitation constant is a function of gravitation energy of a rotating object, more precisely, a function of its rotation frequency”.

The author affirms the statements as valid and proved by laboratory experiments.

Thus we have two values, which  $10^{40}$  times differ from each other and are needed to be combined by one simple expression. There is

$$\gamma_{loc} = 2k\gamma_0\omega^{32}, \quad (89)$$

where  $\gamma_0 = \frac{1}{137}$ , and  $k$  is a parameter of the form of  $0.5 \leq k \leq 1$ .

From the point of view of the expression (89), both the Earth gravitation constant and the electron gravitation constant are not world constants, i.e. the initial constants, which involve all the natural objects. They are local constants, i.e. for the particular Earth and for the particular resting electron. In our opinion, the initial constant is the hyperfine structure constant of  $\frac{1}{137}$ . However, here a difficulty

concerning dimension appears. Nevertheless, the more important thing should be chosen, i.e. the gravitational technics or observing the proprieties.

In this moment we have chosen the technics! Probably, then more forcible arguments will be bound out. Now let us make a numerical testing of that controversial equation (89).

a) For the electron

As the electron is non-spherical let us suppose  $k=0.7$ .

The angular frequency of the electron as a spheroid of  $\frac{r_0}{2}$  mean radius, which rotates at  $c$  tangential speed, is equal to

$$\omega_x = \frac{2c}{r_0} = \frac{3 \cdot 10^{10}}{1.4 \cdot 10^{-13}} = 2.14 \cdot 10^{23} c^{-1},$$

$$\omega_x^{3/2} \cong 99 \cdot 10^{33} c^{-3/2}.$$

Hence

$$\gamma_e = \frac{1}{137} \cdot 2 \cdot 0.7 \cdot 99 \cdot 10^{+33} = \frac{138}{137} \cdot 10^{+33} \cong 10^{+33} cm^3 / g \cdot sec^2. \quad (90)$$

b) For the Earth

According to the same cause as for the electron,  $K=0.7$ .

$$\omega_x \cong 0.725 \cdot 10^{-4} c^{-1}$$

$$\omega_x^{3/2} \cong 61.6 \cdot 10^{-8} c^{-3/2}$$

Let us substitute the index in the equation (89) by these data:

$$\gamma_E = \frac{1}{137} \cdot 1.4 \cdot 61.6 \cdot 10^{-8} = 0.63 \cdot 10^{-8} cm^3 / g \cdot c^2. \quad (91)$$

The result is astonishing. However we will not do hasty conclusions!

To explain the fact of the Earth magnetism existence it is necessary to assume that the Earth core rotates faster than the earth mantle does. From our point of view, the proper gravitation field of the Earth is generated by its inner part, which is fast moving. Observing the relation of  $\frac{m^2}{r}$  it is evident that at  $M_x \cong 0.708M_E$  and  $r_x \cong 0.5R_E$  there is the following relation:

$$\frac{M_x^2}{r_x} \cong \frac{M_E^2}{R_E}, \quad (92)$$

where  $M_E$  is the general mass of the Earth,

$M_x$  is the mass of the rotating core,

$R_E$  is the full radius of the Earth,

$r_x$  is the radius of the rotating core.

In this case the proper gravitation energy of the Earth is defined by the equation:

$$W = \gamma_E \frac{M_E^2}{R_E} = \gamma_c \frac{M_x^2}{r_x}. \quad (93)$$

Hence it is easy to calculate the angular speed of the rotating Earth core. Actually, from the equations (93) and (89) we derive:

$$\frac{\gamma_c}{\gamma_E} = \frac{6.67 \cdot 10^{-8}}{0.63 \cdot 10^{-8}} = 10.6 = \frac{\omega_c^{3/2}}{\omega_E^{3/2}}, \quad (94)$$

hence

$$\omega_E = (10.6)^{2/3} \cdot \omega_c \cong 4.8\omega_c.$$

Thus if it is supposed that the Earth core radius is equal to  $\frac{R_E}{2}$  and its mass is equal to  $0.708 M_E$  then the Earth core rotates 4.8 times faster than the Earth crust! This conclusion does not conflict with the modern concepts of geophysics about the origin of the Earth magnetism!

Let us form combined equations:

$$\begin{cases} M_0 = M_M + M_c \\ \frac{M_x^2}{R_x} = const = \frac{M_0^2}{R_0} \end{cases}, \quad (95)$$

Denoting the core radius as  $X$ , and densities as  $p_0, p_1, p_2$  we derive:

$$p_0 \cdot V_0 = p_1 \cdot V_1 + p_2 V_2,$$

where  $V_0 = 1 = \frac{4}{3}\pi R_0^3$ ;  $V_1 = \frac{4}{3}\pi(1 - x^3)$ ;  $V_2 = \frac{4}{3}\pi x^3$ , or

$$\begin{cases} p_0 \cdot 1 = p_1(1 - x^3) + p_2 x^3 \\ \frac{(p_2 x^3)^2}{x} = \frac{p_0^2 \cdot 1}{1} = p_0^2 \end{cases}. \quad (96)$$

If **the rotation of only the core** is taken into account then at the Earth average density of  $p_0 = 5.5 \text{ g/cm}^3$  the solution of the equation (96) produces:

$$\begin{aligned} X &= 0.548R_0 \\ M_c &= 0.742M_0 \\ p_1 &\cong 1.7 \text{ g/cm}^3 \\ p_2 &\cong 25 \text{ g/cm}^3 \end{aligned}$$

Now we can explain the effect of the Earth Dynamo as the ordinary Barnett effect on condition that the core consists of the elements of the iron group, and both Curie temperature ( $T_c$ ) and the pressure increase faster than the natural temperature, i.e.

$$\frac{\partial T_c}{\partial p} \frac{\partial p}{\partial R} > \frac{dT}{dR}.$$

From the point of view of the modern theory of magnetism it is quite possible. [6]

Naturally, the substitution of the index by a new angular speed value produces the usual value of the Earth gravitation constant of  $6.67 \cdot 10^{-8}$ ; however, now it is not the world constant but just a local one. The extensive material concerned measuring of gravitation constants near different planets of the Solar System is represented in the work [7], and the results of land measuring, which were made near large masses, are shown in the work [8]. These data prove our point of view. Now after defining of the local gravitation constant we can place it into Newton's equation of gravitation energy:

$$W = \gamma \frac{m^2}{r} = 2k\gamma_0\omega^{3/2} \frac{m^2}{r} \approx 1.46 \cdot 10^{-2} k\omega^{3/2} \frac{m^2}{r} \text{ erg.} \quad (97)$$

We have succeeded in introduction of rotation into the gravitation energy. The equation (97) is quite simple and is easy to be experimentally tested.

c) Gravitation energy of a rotating gyroscope

We suppose a precessing gyroscope to concern gravitation. The equation of precession of a classical gyroscope first was formulated by N.E. Zhukovsky. The nowadays it is written as

$$\frac{d\bar{L}}{dt} = [\bar{L} \times \bar{\Omega}], \quad (98)$$

where  $\bar{L}$  is the proper momentum of a gyroscope ("spin"),  
 $\bar{\Omega}$  is the angular speed of a precession.

This equation describes the twisting moment of reaction forces, which appear at any attempt to change the orientation of the gyroscope axis. However, the nature of these forces is not explained by this equation. Let us assume that this equation is the equation of gravitation energy at the same time (by the way, the right part of the equation (98) is evaluated in ergs and expresses the law of conservation of gravitation energy in a mechanical system). If this is the case then we can represent it in another way:

$$W = \xi [\bar{L} \times \bar{\Omega}], \quad (99)$$

where  $\xi = W_{gr} / W_{kin}$  is a gravimechanical relation, which is equal to the relation of the proper gravitation energy of a rotating gyroscope to its kinetic energy:

$$\xi = \frac{2k\gamma_0\omega^{3/2} m^2 / r}{\frac{kmr^2\omega^2}{2}} = \frac{4\gamma_0 m}{r^3 \omega^{1/2}}. \quad (100)$$

Here we suppose the parameter of the form of the gyroscope to be the same for both the equation of gravitation energy and the equation of kinetic energy. Then the final variant of the equation of gravitation energy for a precessing gyroscope is

$$W = \frac{4\gamma_0 m}{r^3 \omega^{1/2}} [\bar{L} \times \bar{\Omega}]. \quad (101)$$

Let us observe the precession of the collective spin at non-linear ferromagnetic resonance at SHF. In the equation (99) we make a usual substitution of variable values:

$$\left. \begin{aligned} \bar{M} &= \gamma \bar{L} \\ \bar{\Omega} &= \gamma \bar{H} \end{aligned} \right\}, \quad (102)$$

where  $\bar{M}$  is matter magnetization,  
 $\bar{\Omega}$  is Larmor precession frequency.  
 $\bar{H}$  is the outer magnetic field

$\gamma = \frac{e}{mc}$  is a magnetomechanical relation.

Then the equation (99) becomes:

$$W = \xi_1 [\bar{M} \times \bar{H}], \quad (103)$$

however  $\xi_1 \neq \xi$  as it causes the gravimagnetic relation for a particular electron.

$$\xi = \frac{W_{gr}}{E_{kin}} = \frac{m_0 c^2}{\alpha} \frac{1}{S \frac{\omega}{2}} = \frac{m_0 c^2}{\alpha} \frac{2\alpha \cdot 2}{m_0 c r \cdot \omega} = 4 \quad (104)$$

where  $\omega r = c$ .

Let us rewrite the expression (103):

$$W = 4 [\bar{M} \times \bar{H}]. \quad (105)$$

Gravitational power, which is radiated at NFMR (non-linear ferromagnetic resonance), is equal to:

$$W = 4MH \cos \gamma \frac{d\gamma}{dt}, \quad \bar{M} = const; \quad \bar{H} = const; \quad (106)$$

$$\varphi \rightarrow 0; \quad \cos \varphi \approx 1.$$

Denoting the ferromagnetic relaxation frequency as  $\frac{d\varphi}{dt} = \omega_r = \frac{2\pi}{\tau_r}$ , and Larmor precession period as

$T = \frac{1}{f}$  we derive the equation of gravitation energy, which is radiated for one precession period:

$$\frac{d\bar{M}}{dt} = -\gamma [\bar{M} \times \bar{H}] - \frac{\alpha\gamma}{M_0} [\bar{M} [\bar{M} \times \bar{H}]] - \frac{8\pi\gamma}{\tau_r f} (\bar{M}\bar{H}) \frac{\bar{M}}{M_0}. \quad (108)$$

Nobody has yet taken into account that the gravitation mechanism of energy dissipation at NFMR is as powerful as “Landau dissipation”.

Thus we have four basic gravitational equations, i.e. (87), (97), (101), and (108). The modeling of the electron has been made to derive these equations. Surely, these equations are just zero approximation. It is impossible to make any laboratory investigation without this approximation on condition of absence of strict solution of these problems. Nevertheless, even at this point the equations predict powerful visible effects, which are of interest of real practice. For clearness let us summarize them in the shareable Table 3. An experiment will demonstrate whether the equations are valid. If the result of

the general experiment is positive then we must raise a question about the possibility of creation of technics of a new type, i.e. gravitonics, and start this work just now.

Table 3

**List of physical mechanisms, which describe powerful gravitation radiation**

№	Mechanism of generation	Equation of radiated power	Coment
1	Ferromagnetic remagnetization	$W = \frac{1}{\alpha} \frac{d}{dt} (BHV) = \frac{1}{\alpha} \frac{d}{dt} \left( \frac{B^2 V}{\mu} \right)$	It has not been observed as a mechanism of gravitation radiation
2	Gyroscope rotation	$W = 2k\gamma_0 \frac{d}{dt} \left( \omega^{3/2} \cdot \frac{m^2}{r} \right)$	For comparison: $W = \frac{m^2 r^4 \omega^6}{c^5}$ L.D. Landau, E.M. Lifshits “Field Theory”
3	Gyroscope precession	$W = \frac{4\gamma_0 m}{r^3} \frac{d}{dt} \cdot \left  \left( \frac{1}{\omega^{1/2}} [\bar{L} \times \bar{\Omega}] \right) \right $	Classical mechanics denies the possibility of non-relativistic mechanical system
4	Magnetization precession	$W = \frac{8\pi}{\tau_r f} (MH)$	The full equation of magnetization precession is $\frac{dM}{dt} = -\gamma [\overline{MH}] - \frac{\alpha\gamma}{M_0} [\overline{M} [\overline{MH}]] +$ $+ \frac{8\pi\gamma}{\tau_r f} (\overline{MH}) \cdot \frac{\overline{M}}{M_0}$

## Part II

### Experimental Testing of New Gravitational Equations

#### Chapter 1

##### Experimental testing of mechanical gravitational equations

###### § 1. Problems of speed of gravitation radiation propagation

Everything represented in this chapter is made by us ourselves (from the idea of the experiment to the complete regulated experimental device). However the conditions of this work realization are worth to a particular report enclosing original documents, or it would be difficult to believe in!

A. Einstein postulated in his works that the speed of gravitation energy propagation (of disturbance, of signal) is equal to the light speed  $c$ . We will not discuss why he did it. Let us turn to opinions of other experts of this issue, whose competence and scientific authority are doubtless.

- a) Isaac Newton, the author of the modern mechanics and of the law of gravity stated: “The speed of gravitational interaction propagation is equal to infinity”. The modern astronomy supports this point of view motivating it by contrary. If the speed of the propagation differed from infinity then the law of gravity would have become:

$$F\left(t - \frac{r}{v_g}\right) = f \frac{m_1 m_2}{[r(t)]^2} \quad (109)$$

and the interaction would have lagged by the value of

$$\Delta t = \left(t - \frac{r}{v_g}\right) \quad (110)$$

that has not been observed in conditions of real stellar observations (see [9]).

- b) In 1787 P.-S. Laplas demonstrated that to determine the laws of planetary motion it is enough to appeal to Newton’s and Kepler’s laws neglecting the gravitational interaction lag. Taking into account the inaccuracy of his time observations, Laplas calculated that the speed of the gravitational interaction is 50 million times exceeds the light speed [10]. Therefore, according to Laplas, the lowest value of the speed of the gravitational interaction is equal to  $1.5 \cdot 10^{18} \text{ cm/sec}$ .
- c) V.A. Dubrovsky [11] observing the issue of longitudinal and transverse wave propagation in the resilient vacuum (the new name of the world aether) came to the conclusion that the speed of the longitudinal waves propagation comes to  $10^9 C$ , i.e.  $3 \cdot 10^{19} \text{ cm/sec}$ .
- d) V.A. Atsyukovsky observing sound propagation in the resilient aether obtained the speed value of about  $6.6 \cdot 10^{31} \text{ cm/sec}$ . Both Dubrovsky and Atsyukovsky identify these waves with gravitational ones [12].
- e) At last, Professor V.B. Braginsky, the main expert of Academy of Science of the USSR of experimental gravitation, officially declared: “It has been ascertained with great accuracy that the speed of gravitation wave propagation differs from the light speed only by third digit...”.

Now let us declare our point of view for this issue. The modern science knows only two types of matter, i.e. electromagnetic matter and gravitational one. The modern physical world picture is a picture of the electromagnetic world and the electromagnetic matter. We know practically nothing about the gravitation matter disregarding those rough mathematical exercises, which does not cause any practical result. Nobody can guarantee that there are no more complicated kinds of matter than the two listed. There can be a great number of unknown kinds of matter. It is not excepted the fact that every kind of matter would have its own set of world constants, which correlate with each other by any way producing a hierarchy of world constants. The hierarchy would include a hierarchy of fundamental speed values of  $c^1, c^2, c^3, c^4, \dots, c^n$ , where  $c^1$  is the light speed, which is equal  $3 \cdot 10^{10}$  cm/sec,  
 $c^2$  is the fundamental speed of the gravitational matter of  $9 \cdot 10^{20}$  cm/sec,  
 $c^3$  is the fundamental speed of “prior matter”, i.e. “resilient aether”, which is equal to  $2.7 \cdot 10^{31}$  cm/sec (for comparison, according to Atsyukovsky, it is equal to  $6.6 \cdot 10^{31}$  cm/sec),  
 $c^4$  is for “X” matter, which is equal to  $8.1 \cdot 10^{41}$  cm/sec ... etc.

Thus the question of the speed of the gravitation propagation is very difficult. Especially it should be taken into account that if the value of propagation speed is changed in Einstein’s equations then both the equations and the very theory are changed as well (here I quote from V.B. Braginsky!). Let us suppose the true value of the speed of gravitational disturbance propagation to lie between Newton’s estimate and Laplas’ estimate, i.e.

$$10^{18} \text{ cm / sec} \leq v_g \leq \infty . \quad (111)$$

How can such huge speed be measured? What size should the measuring instrument be of to validly evaluate such speed to within one order (not to mention the technically admissible inaccuracy of  $\pm 10\%$ )? Let us assume that we have a pulse oscillator and two sensing receivers of gravitation radiation. We observe the distance, which is maximal possible in land conditions, i.e. the distance of “the Earth – the Moon” (about 300 000 km), start the receivers by the same momentum, and measure the momentum lag at this distance by two synchronized atomichrons. If Newton is right then this measuring is senseless! If Laplas is right then the lag comes to  $2 \cdot 10^{-8}$ , i.e. a measurable value. If Dubrovsky is right then the value is of  $10^{-9}$  sec. order. If Polyakov is right then nobody can guarantee the validity of this measuring at the lag of  $\approx 3 \cdot 10^{-11}$  sec (the instability limit of a very atomichron). To work out measuring instruments it is necessary to know the parameters of this radiation, or nobody will appropriate for such a work. We propose an indirect way of measuring of the propagation speed of an unknown radiation as a way out of this impasse, i.e. it can be measured according to the recoil momentum of the very oscillator. To achieve this aim it is necessary for the radiation to be monodirected. It is not important whether it would be strictly focused or not. A quite powerful oscillator is necessary but a receiver is not needed at all.

As it has been demonstrated in Part I, we have a set of gravitation equations, which have been unknown until now. These equations predict powerful mechanisms of the gravitation radiation. Testing of these equations is a fundamental and prestigious matter. Therefore we can produce such an oscillator and measure the speed of this radiation propagation (if it really exists).

## **§ 2. Method of measuring of the speed of an unknown radiation propagation according to the recoil momentum.**

Let us assume that we have some device, which principle of operation is unknown. It is fed by 50 Hz power system and generates some monodirected radiation (X radiation).

Fig.14

Scheme of the speed of X radiation according the “recoil” momentum.

According to Fig.14, this oscillator of  $M_1$  mass must be acted by the recoil momentum  $P_1$ , which is opposite directed, and obtain  $V_1$  speed.

Let us assume the speed of this radiation to be a fundamental value, i.e. the world constant.

Let us write the radiation momentum and the recoil momentum:

$$\begin{aligned} P_1 &= M_1 V_1 & M_1 &= const \\ P_2 &= M_2 V_2 & V_2 &= const \end{aligned} \quad (112)$$

and the law of momentum conservation:

$$M_1 V_1 = M_2 V_2. \quad (113)$$

Differentiating both the parts of the equation (113) by time we derive:

$$M_1 \frac{dV_1}{dt} = M_1 a_1 = F = V_2 \frac{dM_2}{dt}. \quad (114)$$

This X-rays oscillator does not expend its mass in the process of operating as it is just a transformer of electric power into X-rays. Therefore the expendable mass can be defined by the expression of

$$M_2 = \frac{E_x}{c^2}, \quad (115)$$

where  $E_x$  is consumable electric power,  
 $c$  is the light speed.

Hence, the expenditure of the electric power mass is:

$$\frac{dM_2}{dt} = \frac{1}{c^2} \frac{dE_x}{dt} = \frac{1}{c^2} E_x, \quad (116)$$

where  $E_x$  is the consumable electric power.

Now let us revise that this X oscillator is just a transformer therefore, according to the law of matter conservation we can write:

$$\frac{dm_x}{dt} = \frac{1}{c^2} (\dot{E} \cdot \eta), \quad (117)$$

where  $\eta$  is the transformation output.

The product, which is in the brackets in the right part of the equation (117), is the power of  $X$  radiation, which we denote as  $W$ . Now we can write the final expression of the propulsion force of this “black box”:

$$F = \frac{V_2}{c^2} W = \frac{V}{c^2} W . \quad (118)$$

The author begs pardon for such detailing; however, as practice has shown, the primitiveness of this method accompanied by its effectiveness causes irritation and lack of understanding. The equation (118) is quite unexpected. If there are  $F$  force evaluated in grams and  $W$  power evaluated in watts then their relation (i.e. specific impulse) becomes:

$$\frac{F}{W} \approx 10^4 \frac{V}{c^2} g / Wt . \quad (119)$$

Now let us suppose what the equation (119) can produce at different speeds of  $X$  radiation.

a) **“Photon rocket”**:  $V = c, \frac{F}{W} \approx \frac{10^4}{c} = 3 \cdot 10^{-7} g / Wt$ . Hence, photon starprobe vehicles are impossible to be created as even at the monodirected power radiation of 1MWt the propulsion comes to just 0.3 grams.

b) If the speed of the propagation is equal to  $10^9$  then there is  $\frac{F}{W} \approx \frac{10^4}{30} \approx 330 g / Wt$ .

It is interesting.

c) If the speed is equal to  $3 \cdot 10^{10} C$  then  $\frac{F}{W} \approx 10^4 g / Wt$ . From the point of view of technical policy, the cited values are a very forcible argument as at  $V = c$  the communication by gravitation waves is of academic interest. Moreover, space engines are unnecessary even if their output is equal to one! Nevertheless, both the unlimited communication (within our Universe) and powerful gravitational engines requiring only the electric power, which operate at  $3 \cdot 10^{10}$  speed, are needed. According to rocketeers’ mind, the momentum of such an engine is equal to  $10^{18} c$ , and at mass outflow velocity of just 1 gram per a second the propulsion comes to  $F \approx 10^{12} T$  [13]. That follows from the equation (119). Surely, it is the maximal estimate for the engines, which can never be achieved. Nevertheless, supposing this estimate to be 2-3 orders less it would be enough to reach the nearest stars in the next century.

Thus the problem of the propagation speed is not a scholastic debate of practice experts and theorists but a fundamental matter, which has a huge practical potential.

Now let us turn to the real practice. For purity of the experiment the oscillator must radiate nothing but the gravitation energy. From this point of view a mechanical oscillator is most suitable for us as it is well-known that mechanical non-relativistic systems radiate nothing. It was found out in 1975, and we are the only people not to know it. However, we know mechanical equations, which describe this radiation. For example:

$$W = 2k\gamma_0 \omega^{3/2} \frac{m^2}{r} , \quad (97)$$

which is the equation of the gravitation energy of a rotating mass, and

$$W = \xi \left[ \overline{L} \times \overline{\Omega} \right], \quad (99)$$

which is the equation of the gravitation energy of a precessing gyroscope. These equations produce six different ways of the gravitational power radiation in non-stationary mode of the mechanical systems operation.

The following parameters can be regulable: the proper frequency of a gyroscope, the mass of a gyroscope, the radius of a gyroscope, the momentum of a gyroscope, a precession frequency, the precession angle of a gyroscope. Naturally, we must ensure the modulation due to a particular law of only one parameter maintaining the stability of the others. However, according to practical reality, it is possible to be ensured.

Let us turn to the equation (118)

$$F = \frac{V}{c^2} W.$$

If we succeed in valid measuring of the propulsion force  $F$  and all the dynamic parameters of magnitudes, which are included into the equation of a concrete mechanism of generation  $W$ , then the relation of  $\frac{F}{W}$  will produce an experimental value of the propagation speed evaluated in  $V/c^2$ . It is evident that the dimension of  $V/c^2$  becomes sec/cm in SGS system. Hence the propagation speed has a normal dimension, i.e. cm/sec.

First measuring of the propagation speed of the gravitation radiation was made by the author in 1984 and reported at a physical seminar of IPF of Academy of Science of the MSSR, and at SPP of the presidium of Academy of Science of the USSR in the same 1984. Since these results were retested in 1985-1984 at a higher level taking into accounts all the discussions of the subject. Now we will not dwell on those discussions, just mention that the result obtained in 1984, which produce the estimate of  $V/c^2 \approx 10^{-2}$  (sec/cm) is right, i.e. it has been proved in a wide diapason of operation modes of a system of gyroscopes, which is precessing at angular acceleration.

Comparison of all these experimental materials belonging to the time interval of 1985-1986 causes a conclusion that we deal with two different types of radiation, which are conditionally called a dipole radiation and quadrupole radiation. The dipole radiation is generated by a mechanical system, which does not change its geometries during the working cycle. The quadrupole radiation is produced by a system of changeable geometry. Hence their measured values of the propagation speed are almost 100 times differ from each other. Only the propagation speed of the **quadrupole** radiation proves the author's prediction, i.e.  $V/c^2 \approx 1$ . For the dipole radiation it is observed inverse dependence on the frequency that is demonstrated at the observation of experimental results below. It is yet incomprehensible if there is some regularity or it is the result either of the output frequency dependence of the generator or of a function of the radiation direction. The results, which have been obtained for the quadrupole radiation, are stable.

### § 3. An experimental device description

The experimental device designed for measuring of the propagation speed of the gravitation radiation consists of three fundamental units:

- a) a sensitive balance, which has one degree of freedom,

- b) a system of indication of weight small changes
- c) a force assembly, i.e. a mechanical system, which changes its weight in a dynamic mode.

A general view of the experimental device is represented in Fig.15, 16. Let us observe the experimental device in details.

a) The balance (Fig.15)

The balance consists of an unmovable part and a movable one. The unmovable part of the balance is formed by a system of three rods of stainless steel (1), which are fastened in special yokes (2) built in the floor and the ceiling of a premise. The rods are aligned according to an adjusting tool, variation from plumb does not exceed 5 angular minutes. On the rods (1) close to the low yoke of the balance (2) there are permanent magnets (3), which ensure a magnetic suspender of the body of the movable part of the balance (4). The movable part of the balance is centralized on the rods (1) by 18 ball-bearings (i.e. 6 ball-bearings are radial, and 12 ones are tangential). Permanent magnets (5), which generate magnetic field oppositely directed relatively the system of the magnets (3), are fastened to the low part of the body. Thus at any load in a quiescent mode the weight of the movable part is completely compensated by forces of magnetostatic interaction of the permanent magnets (3, 5) that allows immediately measure the weight increase of the dynamic system. There is a device, which ensures five powering loads and one monitor signal selection that greatly decreases the balance sensitiveness. Nevertheless the balance ensures the sensitiveness of  $10^{-4}$  order of a full weight of the loaded movable part under trying conditions of permanent axial and sharing overloads.

Fig.15

The general view of the experimental device: 1 – directing rods, 2 – supporting plates, 3, 5 – permanent magnets of the suspender, 4 – the body of the movable part of the balance, 6 – a measuring scheme, 6a – the metric pin with a ferrite head, 7 – a cylindrical mirror of indication optical scheme, 8 – the dynamic block (“engine”).

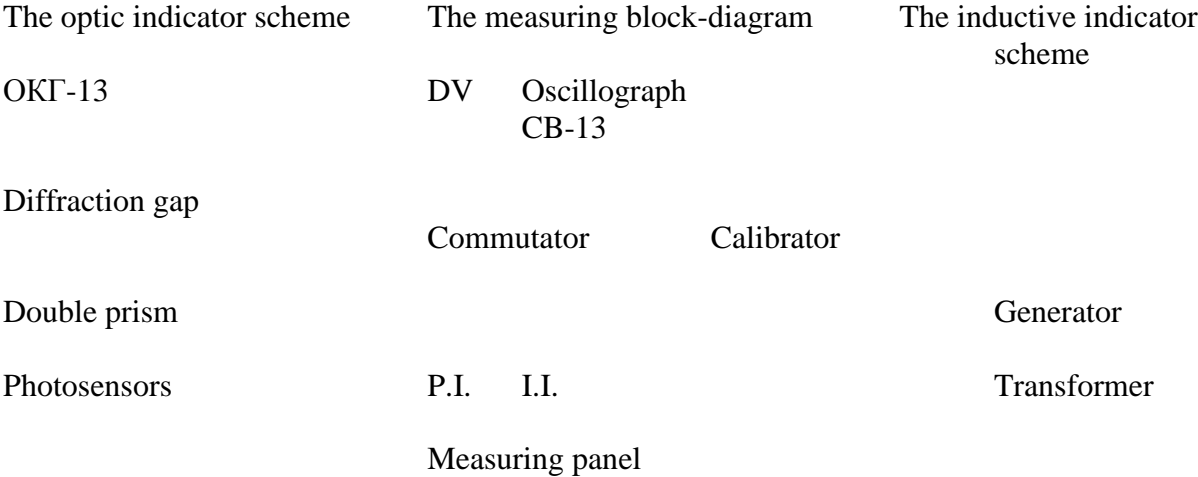
b) The systems of weight increase indication

Actually, the task comes to measuring of small axial displacements of the balance in a dynamic working mode of the force aggregate. In the experiments two independent indicators of small axial displacements of a balance were used, i.e. an inductive indicator (6; 6a) and an optic indicator (7). The inductive indicator is fastened on the low iron yoke (2) and operated by a ferrite rod, which is connected with the movable part of the balance (4) by a plexiglass rod (6, a). The cylindrical mirror of the optic indicator (7) (it is covered by a special casing, which preserves the mirror from scattered light) is placed on the low part of the body (4) of the movable part of the balance. The general view of the balance, of the measuring block, and of the measuring scheme is represented in more details in Fig.16 and does not require additional explanations.

It should be noted that in spite of the higher sensitiveness of the optic indicator it has been refused later on since the mentioned tendency to develop transverse force effect as a longitudinal one. In

Fig.16 a notation of PI means photo signal intensification, and a notation of II means inductive signal intensification, DV means a digital voltmeter.

a



b

Fig.16  
Measuring instruments (*a* and *b*).

An electrical scheme and the principle of operation of the inductive indicator are represented in Fig.17.

Fig. 17  
Scheme and the principle of operation of the indicator of a balance displacement.

It is necessary to note one more important circumstance. Since the balance sensitiveness is defined by a quality of the suspender system then we need the suspender system to have maximal good quality. However, on other hand, at good quality any impact disturbance of the balance produces mechanical auto-oscillations, which mask a useful signal. Thus the obstacle increases as well as the balance sensitiveness does. To eliminate this contradiction a special electric filter, which allows filter the auto-oscillations, was designed. It is demonstrated in Fig. 18.

Fig.18  
Auto-oscillations filter of the balance

The designed measuring instruments allow simultaneously display up to four signals on the oscillograph screen, i.e. the signals of the propulsion force, of the proper frequencies of gyroscopes, of the precession frequency, of time marks etc.

c) The force aggregate

In the process of work the following generation mechanisms were investigated.

1. A massive gyroscope rotation, which has a positive angular acceleration, in the mode of “acceleration – hard breaking”. The measuring was made at the acceleration path.
2. The precession of the system consisting of four gyroscopes in the mode of p.1.
3. The precession of the system of four gyroscopes, which have a variable precession angle.
4. Effects of hard breaking of a heavy gyroscope.

As every of the force aggregates require explanations let us observe them taken separately.

#### § 4. A gyroscope multipole of “Bouquet”

The force aggregate is a system of four gyroscopes equipped with a drive from D-25M engines, which are placed a common yoke. Every drive is at the angle of 35° relatively the common precession axis. The precession of the system of the gyroscopes is provided with a special mover, which is a worm-and-wheel gearbox equipped with an outlet at a tread flange.

The general view of the aggregate is represented in Fig. 19; 20.

Fig.19

A force aggregate in assembling

Fig.20

Mover: 1 – a plate, 2 – a reducer, 3 – the body of gyroscopes yoke, 4 – the reducer drive, 5 – the reverse-switch, 6 – the tread flange

Possible operation modes are demonstrated in Fig.21, where there is the decoding of notations accepted in Fig.22; 23. Four different operation modes are possible:

1. **The gyroscopes are switched off.**  $\omega = 0, L = 0, \frac{d\Omega}{dt} > 0$  (Fig.21 (1)).

In this case the yoke of gyroscopes (3) rotates like a blank, and we deal with the simplest case of rotation of a massive gyroscope, which has the angular acceleration. A direction of a propulsion momentum  $F_1$  is shown by an arrow and depends on the direction of the blank rotation. The exchange of the yoke (3) by an equivalent massive gyroscope (of equal radius and mass) can not change the case. In this case we deal with the gyroscope accelerated rotation, which has zero initial velocity. The angular velocity of the precession  $\Omega$  (in this case it is the rotation speed of the massive gyroscope) is continuously controlled. Thus if we know the parameters of M and R and has measured the propulsion momentum of  $F_1$  then we can calculate the relation of  $V/c^2$  :

$$\frac{V}{c^2} = \frac{F_1}{W_1} = \frac{F_1}{3k\gamma_0\Omega^{1/2}} \cdot \frac{R}{M^2} \cdot \frac{dt}{d\Omega}. \quad (119)$$

At switching of the gyroscopes on we can see a summary effect of

$$F = F_1 + F_x, \quad (120)$$

where  $F_x$  is the propulsion momentum, which is defined by a switch method and a mode of powering of the system of the gyroscopes.

## 2. The gyroscopes are switched on (next nearest)

In Fig.21 (2) one of the most interesting results, from our point of view, is represented. In this case the direction of the proper rotation of the gyroscopes is chosen as “next nearest”, i.e. either of the two nearest gyroscopes rotates in the opposite direction. If the angular velocities are equal, i.e.  $\omega_1 = \omega_2 = \omega_3 = \omega_4$ , and the moments are equal as well, i.e.  $L_1 = L_2 = L_3 = L_4$ , then the sum of their projections on the precession axis and on the precession flat is equal to zero, i.e.  $(\sum L)_0 = 0 = (\sum L)_p$ . Nevertheless, in this case an inexplicable, on our mind, propulsion effect is observed. In Fig.21 (2) it is marked for the propulsion force of

$$F_2 = \frac{V}{c^2} W^2 = \frac{V}{c^2} (W_1 + ?). \quad (121)$$

Fig.21

The mode of operation of the gyroscope system

## 3. The gyroscopes are switched on (all of them are in the same direction; see Fig.21 (3))

In this case the sum of the projections on the precession flat is  $(\sum L)_p = 0$ , and the sum of the projections on the precession axis is  $(\sum L)_o = \max, \frac{d\Omega}{dt} > 0$  as well as in all the other cases.

Here the propulsion effect is produced by two effects:

$$F_3 = \frac{V}{c^2} \left( \xi \left[ \bar{L} \times \frac{d\Omega}{dt} \right] \pm W_1 \right) \quad (122)$$

that should be taken into account at calculation of  $V/c^2$ .

#### 4. The gyroscopes are switched on in pairs (Fig. 21 (4))

Here every pair of the gyroscopes rotates in the direction, which is opposite to the rotation direction of another pair. In this case  $(\sum L)_p = 0$ , and  $(\sum L)_o = \max$ . The precession, which angular acceleration is  $\frac{d\Omega}{dt}$ , produces the effect of

$$F_4 = \frac{V}{c^2} \left( \xi \cdot 4L \frac{d\Omega}{dt} \sin 35^\circ \pm W_1 \right). \quad (123)$$

The basic results obtained for the multipole of “Bouquet” are represented in Fig. 22 and 23, which have been formed according to the results of oscilloscope photography.

Fig.22

Dynamic parameters of the gyroscope multipole

Fig.23

Dynamic parameters of the gyroscope multipole at a forced precession, which has the angular acceleration.

In Fig. 22 (1) the testing of calibration mars is represented. In Fig.22 (2) (a, b) a pattern of changing of the precession angular velocity of a yoke of the gyroscopes  $\Omega$ , which occurs for one operation cycle

of the device. Here every period of a sinusoidal signal is equal to  $\frac{1}{20}$  of the full turn of the yoke that allows evaluate the instantaneous value of  $\Omega$  and of  $d\Omega/dt$  in practically any point of the oscillogram. In Fig. 22 (3) the propulsion moments  $F$  of the angular velocity  $\Omega$  for both the right precession and the left precession of the blank are simultaneously represented. The index of “9” means the number of series of pictures. As it can be seen from the pictures, a superposition of the patterns impedes their decoding. In Fig.22 (4) (a, b) the analogous results (i.e. the blank rotation) is demonstrated without an oscillogram of the angular velocity  $\Omega$ . In Fig.22 (4) a contour of an average statistical angular velocity is demonstrated therefore we get a notion of what processes occur in each part of the operation cycle. By the way, it can be seen from the pictures that the angular velocity  $\Omega$  is quite instable. It is caused by instability of the mover operation (i.e. the worm pair of the reducer), which causes hindrances in the experiment. However, since we begin to investigate the new area then every result is very interesting even if it is just qualitative.

In Fig.23 (5) (a, b) the oscillograms of the right precession and the left precession of the quadrupole are represented. The sum of all the projections of the quadrupole momentum on both the precession axis and the precession flat is equal to zero. Therefore the results, which were obtained for the left precession, have been very amusing. For the left precession the burst of the propulsion force comes to 50 g (the dotted line, which is on the top and on the foot of the oscillogram, i.e. the mark of  $\pm 100$  g).

In Fig. 23 (6) the results obtained for the gyroscopes, which rotate in the right direction, are demonstrated. The results obtained for the gyroscopes, which rotate in the left direction, are represented in Fig. 23 (7) (a, b). Here it is evident that the propulsion momentum of the gyroscopes, which rotate in the left direction, is well-defined for both the precessions. For comparison, it should pay attention to the “blanks” rotation (see Fig.22 (4) (a, b)). At least, Fig.23 (8) (a, b) demonstrates an interesting case, which is decoded in Fig.21 (4).

Here we deal with a precession of a fictitious gyroscope, which rotation axis is perpendicular to a vector of the angular velocity of the precession. This precession, which has the angular acceleration, is unjustly not observed by any theory. In this case the propulsion momentum for the right precession achieves the maximal value of +100 g and exceeds it, and the propulsion momentum for the left precession comes to –80 g. Surely, from the point of view of our nowadays abilities, the demonstrated results are very unimportant. However, they were the first and allowed raise two scientific questions:

1. Whether can the non-linear mechanical system not study anything but heat generated by the friction of bearings?
2. What is the propagation speed of this radiation if it actually exists?

### **Retesting of the results obtained in 1984**

One of the tasks of 1986 was retesting of the results obtained in 1984 by using of a new metrics.

The system of four gyroscopes, which is represented in Fig.19, 20, had to be replaced by an equivalent system of two gyroscopes (Fig.28, b) due to technical causes (6-milimetered axis of D-25M engine was broken because of dynamic overloads). The very experiment had to be restricted to two points of 6 and 7 (see Fig.23). In this case the relation was derived from the expression of

$$\frac{V}{c^2} = \frac{(F_{\Sigma} - F_0)981}{2\xi \left[ \bar{L} \times \frac{d\Omega}{dt} \right]}. \quad (124)$$

At the cyclic frequency of the gyroscopes rotation of  $f = 100\text{Hz}$ , the gyroscope mass of  $m_0 = 775\text{g}$ , and the radius of  $r = 4.4\text{cm}$ , and a specified precession angular of  $\alpha = 35^\circ$  there is

$$L = \frac{mr^2}{2} \omega \frac{775 \cdot 19.2}{2} \cdot 628 = 46.6 \cdot 10^5 \text{ g} \cdot \text{cm}^2 / \text{sec}$$

$$\xi = 4\gamma_0 \frac{m}{r^2 \omega_0^{1/2}} = \frac{4}{137} \frac{775}{84 \cdot 25.2} = 0.8 \cdot 10^{-2}$$

and finally:

$$\frac{V}{c^2} \Big|_{100\text{HZ}} = \frac{(F_\Sigma - F_0)981}{42.6 \cdot 10^3 \frac{d\Omega}{dt}} = 1.85 \cdot 10^{-2} \frac{\Delta F}{d\Omega/dt}, \quad (125)$$

where  $F_2$  is the summary propulsion of the gyroscope system,  
 $F_0$  is the propulsion effect of the blank.

Since we are interested in just the accelerated part of the precession then the mode of operation has been chosen due to the rotor, which combines the system of the gyroscopes, made the 1/3 of the full turn (120°) can be automatically switched off. We had to refuse photographing of the oscillograms for mass collecting of a set of experimental statistical data. In the process of work the zero of a propulsion indicator systematically shifted that did not affect the differed results of the measurements. The most inaccuracy was caused by the instable operation of the worm pair of the mover (the instability is  $\frac{d\Omega}{dt}$ ).

The general view of the propulsion momentum of the system, which operates in the mode of blank, is represented in Fig.24. The summary propulsion momentum for the right rotation of the gyroscopes is demonstrated in Fig.25. The summary propulsion momentum for the left rotation of the gyroscopes  $\omega_0^+$  is demonstrated in Fig.26.

Let us decode the oscillograms, which are shown in Fig. 24, 25, 26. “250W. left” means that the power load of the mover is equal to 250W, the precession is left; “gyr. 30. left” means that the power load of the gyroscopes is equal to 30W, the rotation is left directed;  $\Delta t$  is the time period from the rotation start to the counting point (propulsion peak  $F$ ),  $\Omega$  is the tops of moments of a tachometer generator of a step of  $\pi/10$  radian. Actually, these tops demonstrate not the very  $\Omega$  value but the turning angle  $\Delta\varphi$  of a mechanical system, which occur for the time period of  $\Delta t$ . At the calculations the maximal values of  $\Omega = \frac{\Delta\varphi}{\Delta t}$  and  $\frac{d\Omega}{dt} = \frac{\Delta\varphi}{(\Delta t)^2}$  were accepted, the scale interval for the propulsion, which is demonstrated in the graphical charts, is equal to 5 g/int., the scale interval for the time period is  $\delta t_0 = 6.25 \cdot 10^{-3}$  sec/mm. Averaged values of  $V/c^2$  for 12 series of the similar measurements (there are 3-5 measurements in every series), which are in the area of  $\omega/2\pi = 100$  are represented in Fig.27. Here the maximal value of  $V/c^2$  insignificantly exceeds  $1 \cdot 10^{-2}$ .

Fig.24

The blank precession:  $\Omega$  is left

Fig.25

The gyroscopes precession  $\Omega$  is left,  $\omega_0$  is right,  $\Delta F = -85.5 \text{ g}$ .

Fig.26

The gyroscopes precession:  $\Omega$  is left,  $\omega_0$  is left,  $\Delta F = +36g$  .

Fig.27

An experimental dependence of  $\frac{v}{c^2} f(\omega)$ , which is demonstrated at impact rotation of the massive gyroscope or at an impact precession of a gyroscope system

## § 5. Investigation of the effects of impact rotation of the massive gyroscope

The effect of the precession, which has the angular acceleration, appeared to be not productive, i.e. no more than 10% of the summary effect, that, first of all, was caused by an insignificant kinetic energy input of the very gyroscopes to the full energy of the force aggregate. Since that the investigation of the dynamic parameters of the massive gyroscope were made. The mass and the radius of the massive gyroscope are equivalent to the analogous parameters of the yoke of the gyroscopes, which was replaced by the gyroscope on the same mover (see Fig.28). Typical oscillograms for the right rotation and for the left rotation of the massive gyroscope are represented in Fig. 29 and 30. Here it is evident that the effect for the left rotation than the effect for the right one. Most likely, it again can be explained by the peculiarities of operation of the worm pair of the mover, which are caused by the fact that its left rotation does not correspond to its right rotation. By the way, the oscillograms of the angular velocity prove this fact.

Fig.28

The massive gyroscope-blank (a), and the gyroscope system (b).

Fig.29

The effect of impact acceleration of the massive gyroscope:  $\Omega^+$  is left,  $\Delta F = +123g$ .

Fig.30

The effect of impact acceleration of the massive gyroscope:  $\Omega^-$  is right,  $\Delta F = -28.5g$ .

The experimental data processing was made by the same way as the previous case; Calibration data for the force  $F$  and the time period of  $\delta/t_0$  are the same (5 g/int.,  $6.25 \cdot 10^{-3}$  sec/mm).

$$\text{At } M=5500 \text{ there is } R = 11\text{cm}, W = 3k\gamma_0\Omega^{1/2} \frac{M^2}{R} \cdot \frac{d\Omega}{dt} = 2.7 \cdot 10^3 \Omega^{1/2} \frac{d\Omega}{dt}, \Omega \approx \frac{\Delta\varphi}{\Delta t}, \frac{d\Omega}{dt} \approx \frac{\Delta\varphi}{(\Delta t)^2}.$$

The final expression for the relation of  $V/c^2$  becomes:

$$\frac{V}{c^2} = \frac{981 \cdot \Delta F}{2.7 \cdot 10^3 \Omega^{1/2} \frac{d\Omega}{dt}} \approx 0.365 \cdot \frac{\Delta F}{\Omega^{1/2} \frac{d\Omega}{dt}}. \quad (126)$$

The results of calculations for 12 series in the area of  $\omega/2\pi = 12c^{-1}$  are represented in Fig.27. As it can be seen from the graphical chart the interval of the results is very great and, evidently, contains some dependence, which clarification is in prospects.

## § 6. The effect of impact break of the massive rotating gyroscope.

A special heavy gyroscope, which mass is 9700g and radius is 11.35cm, was designed for this experiment on the base of the electric engine of SL-661M. The general view of this construction is demonstrated in Fig.31, conditionally named as a “rotor”. Since this gyroscope has great inertia force and one-valuedness of the results of the observations requires the maximal effect then the reverse mode of breaking (powering of the equal load of the opposite polarity) was used in the experiment to the full stop of the rotor. It was controlled according to the signal of the tachometer.

Fig.31

The configuration of the rotor without an external body (a) and with the external body (b). Typical oscillograms are represented in Fig.32 and 33. Every series of changes is processed as well as in the previous case. The final expression for the relation of  $V/c^2$  becomes in this case:

$$\frac{V}{c^2} = \frac{981 \cdot \Delta F_{(g)}}{3k\gamma_0 \Omega^{1/2} \frac{M^2}{R} \frac{d\Omega}{dt}} \approx 1.09 \frac{\Delta F_{(g)}}{\Omega^{1/2} \frac{d\Omega}{dt}} \text{ sec/cm} . \quad (127)$$

The results of seven series of changes in the diapason of  $20 \leq \frac{\omega}{2\pi} \leq 40c^{-1}$  are represented in Fig. 27. In Fig.27 the dotted line does not demonstrate a quantitative dependence of the radiation propagation speed on the rotation frequency of the radiating gyroscope but it rather demonstrates the output of mechanical rotation energy transformation into the radiation. Why is it so? It seems to be in the opposite way!

The results, which are represented in Fig.27, are quite far from the declared value of  $V/c^2 = 1$ . Therefore we dare name all the described mechanisms of rotation by the general term of a dipole radiation. We suppose to obtain to obtain an expected value for the quadrupole radiation, i.e. for a real gravitation radiation.

Fig.32

An oscillogram of the impact breaking of the rotor:  $\Omega$  is right,  $\Delta F = +71g$

Fig.33

An oscillogram of the impact breaking of the rotor:  $\Omega$  is right,  $\Delta F = -106g$

## § 7. A quadrupole generator of directed gravitation radiation (“Yolka” (“Fir-tree”))

A.Einstein introduced the notions of a quadrupole radiation, quadrupole momentum, which are poorly understood by theorists, into Gravics. From our point of view, the quadrupole momentum is a property only of a mechanical system, which changes its geometry for one operation cycle. It can be said more strictly that a solid body, which rotates on any unmovable axis, does not have the quadrupole momentum in its gravitational sense. The results of an experimental investigation of a construction demonstrated in Fig.34 are the basis of this declaration. This construction is a system of four gyroscopes, which are combined by a common yoke in a particular way. In the process of the mechanical cycle realization the simultaneous change of angle of inclination of the gyroscopes axes relatively the common precession axis occurs as well as the very precession relatively the common precession axis does. More over, the construction ensures the possibility of testing and regulating of the operation modes of the very gyroscopes. The device is completely atuomatized, in the opposite case the investigations are impossible to be realized.

Fig.34  
“Yolka”

From the point of view of mechanics this system has three degrees of freedom. The general mass of the construction comes to 32 kg at the general mass of the gyroscopes of 6400 g. Since this construction consists of about 200 elements, which description can make difficulties for comprehension, then we will just describe the possible modes of this gyroscope system. It has four particular basic dynamic operation modes. Nevertheless, there are 24 possible combinations of these modes. Every mode has its own peculiarity and contains a particular charge of information. Thus experimental abilities of this force aggregate are very high.

Thus let us observe the basic operation modes:

### 1. **Swinging of Blanks**

In this case the gyroscopes do not rotate ( $\omega_0 = 0$ ), the precession is absent ( $\Omega = 0$ ), and the precession angle  $\Delta\varphi$  is a variable parameter. Since in this construction a change of the precession angle is accompanied with the displacement of the centre of masses of the gyroscope system along the vertical axis of the system (i.e. the displacement is non-symmetrical relatively the Earth gravity acceleration) then the used balance produces a non-symmetrical response of  $\pm \Delta F$ , as it is shown in Fig.35.

The value of  $\Delta F = -365g$ , which is indicated in the oscillogram, is the real dynamic zero of this system.

“Swinging” of blanks”

Fig.35

### 2. **Swinging of Gyroscopes**

As it is shown in Fig. 36, the case, when the gyroscopes are switched on ( $U_g = 32V$ ), greatly changes the observed pattern. In this case the summary projection of the vectors  $L$  on the precession axis  $\Omega$  changes its value according the following law:

$$L_{\Sigma}(t) = 4L_0 \cos \gamma(t). \quad (128)$$

It follows from this that, according to our theory, a mechanical system must radiate the gravitation energy even in this simplest case. Actually, the expression of  $W = 2k\gamma_0\omega^{1/2} \frac{m^2}{r}$  can easily be transformed into the expression of

$$W = \frac{4\gamma_0}{r^5\omega^{1/2}} L^2 \quad (129)$$

at  $k=0.5$ . For the variable parameter of  $L=L(t)$  at  $\omega=\text{const}$ , and  $r=\text{const}$  the radiated gravitation power is defined by the expression of

$$W = \frac{8\gamma_0}{r^5\omega^{1/2}} L \frac{dL}{dt} . \quad (130)$$

As it can be seen from the oscillogram in Fig.36, there is  $\Delta F = -475 \text{ g}$  for the gyroscope right rotation, and  $\Delta F = -310 \text{ g}$  is for the gyroscope left rotation.

“Swinging” of gyroscopes”

Fig.36

Taking into account the fact that the dynamic zero produces  $\Delta F = -365 \text{ g}$  we can derive the propulsion effect for the right rotation, i.e.  $\Delta F_{\text{right}} = -110 \text{ g}$ , and for the left rotation, i.e.  $\Delta F = +55 \text{ g}$ .

### 3. Precession of Blanks

If the gyroscopes are switched off ( $L=0$ ) then in the mode of the cyclic precession the gyroscopic system behaves as some four-horned gyroscope of a variable radius. The peculiarity of this mode is the fact that its cycle is two-phased, i.e. the precession phase alternates with the phase of “reverse swinging”. Therefore every full cycle ends in the initial position of the system of the gyroscopes, as it is shown in a graphical chart of  $\varphi = \varphi(+)$ . Here are four possible variants of the cyclic operation, i.e.

- a) the right precession, which is convergent, i.e.  $\frac{d\varphi}{dt} < 0$ ;
- b) the right precession, which is non-convergent, i.e.  $\frac{d\varphi}{dt} > 0$ ;
- c) the left precession, which is convergent, i.e.  $\frac{d\varphi}{dt} < 0$ ;
- d) the left precession, which is non-convergent, i.e.  $\frac{d\varphi}{dt} > 0$ .

In Fig. 37 there is an oscillogram of the propulsion momentum, which occurs for the cycle, where  $\Delta F = +175g$  taking into account the dynamic zero. In this case the propulsion momentum is defined by the expression of

$$F = \frac{V}{c^2} W = \frac{V}{c^2} \left[ -2k\gamma_0 \frac{M^2 \Omega^{3/2}}{R^2} \cdot \frac{dR}{dt} \right]. \quad (131)$$

It is easy to understand that the index  $F$  is defined by  $\Omega \pm$  (right – left) as well as by  $dR/dt$  (convergent precession – non-convergent precession). Hence, the resulting propulsion effect can have four different numerical values.

“Precession of Blanks” (right, non-convergent)

Fig.37

#### 4. Precession of Gyroscopes (Fig.38)

If the gyroscopes are switched on then the propulsion effect of the blanks is combined with the propulsion effect of the gyroscopes, which have a variable precession angle. In this case the additional force is defined by the expression of

$$\pm F = \frac{V}{c^2} \cdot \frac{4\gamma_0 m}{r^3 \omega^{1/2}} L \cdot \Omega \cdot \cos \frac{d\varphi}{dt}. \quad (132)$$

Since  $\bar{L}$  is always a new parameter here then the index  $\pm F$  is defined by  $\pm \bar{L}$  as well, i.e. by the direction of the gyroscopes proper rotation (right – left).

If all the effects, which simultaneously act on our balance, are summarized then the resulting oscillogram is defined by the following equation:

$$F = F_1 \pm F_2 \pm F_3 \pm F_4, \quad (133)$$

where  $F_1$  is the swinging of the blanks,

$F_2$  is the swinging of the gyroscopes,

$F_3$  is the precession of the blanks,

$F_4$  is the precession of the gyroscopes,

i.e. the expression (133) describes 15 possible combinations.

However, the analysis of action of each mechanism can be simplified in a particular way. To achieve this aim the resulting effect of the motion of simpler type (for example, of swinging of the blanks) should be accepted as the dynamic zero of the motion of more complicated type (of precession of the blanks) etc.

“Precession on gyroscope” (right, convergent)

Fig.38

## § 8. Experimental results for the quadrupole generator

In Fig.39 the results of investigation of the blanks precession effect deducting the blanks swinging effect. Here the force  $F$ , which is declared as evaluated in “relative units”, in fact, is given in grams deducting 80g caused by deteriorated powering of a phase-metric scheme. At the same time it has been found out that the accuracy of measurement of the angular velocity of the precession  $\Omega$  is low. Therefore on the abscissa axis it was replaced by the voltage of the mover powering (it ensures the precession) without the last zero (now it is really relative units). The curves, which are represented here, are plotted by 5 points each, and the particular point is the average value of the results of ten measuring sessions. Hence, the results of 200 measuring sessions are represented.

Right convergent

Left non-convergent

Left convergent

Right non-convergent

Precession of blanks  
Fig.39

Fig.40

Some asymmetry between the left effects and the right effects can be explained by the asymmetry of the mover operation, which has been mentioned before. The best results (Fig.39) (the precession is right convergent) was used to calculate the relation of  $V/c^2$  according to the principles demonstrated in Fig.40. A tachometer was built in a kinematical system of the quadrupole. The tachometer was a system of eight magnetic elements, which were uniformly placed around the circle of a special plexiglass disk. This disk rotated together with the gyroscopes relatively an unmovable inductive coil.

Moments of EMF-induction are demonstrated in the right top corner of Fig.40, where eight moments correspond to one full turn of the system of gyroscopes relatively the vertical precession axis. All the temporal measuring were made by four moments ( $N=4$  in table 5), and the very time was measured by time involute of the oscillograph.

$\Delta \tau$  is the time period of passing of four moments (the time period of a half of the turn);  
 $dt$  is the time period of the full precession cycle.

The results of the measurements are represented in Table 4.

Table 4

**$V/c^2$  according to parameters of the gyroscope of a variable radius**

$U_T$ , V	$N$	$\Delta\tau$ , sec	$T_{1turns}$	$\Omega$	$dt$ , sec	$\frac{dR}{dt}$	$\Omega^{3/2}$	$\Omega^{3/2} \cdot \frac{dR}{dt}$	$\times 3.21 \cdot 10^3$	$F$ , g	$F \times 981$	$V/c^2$
140	4	0.263	0.526	12.0	1.16	1.5	41	61.5	$1.97 \cdot 10^5$	180	$1.76 \cdot 10^5$	0.895
150	4	0.250	0.500	12.6	1.45	1.2	45	54.0	$1.74 \cdot 10^5$	200	$1.96 \cdot 10^5$	1.13
160	4	0.250	0.500	12.6	1.00	1.75	45	78.5	$2.54 \cdot 10^5$	230	$2.25 \cdot 10^5$	0.885
180	4	0.250	0.500	12.6	1.29	1.36	45	61.2	$2.05 \cdot 10^5$	300	$2.94 \cdot 10^3$	1.43
200	4	0.238	0.476	13.2	1.26	1.39	48	66.6	$2.15 \cdot 10^5$	390	$3.82 \cdot 10^5$	1.77
200	4	0.178	0.374	16.8	1.11	1.59	69	110	$3.56 \cdot 10^5$	480	$4.70 \cdot 10^5$	1.32

Let us observe the last column of the table. If an obvious outbreak, i.e. the value of 1.77, is ignored then the average value of  $V/c^2$  comes to  $1.15 \pm 30\%$ . This can be considered as a satisfactory result at the change of such a huge speed as  $9 \cdot 10^{20}$  cm/sec. It does not raise doubts that the improving of the measurements accuracy (first of all of  $\Omega$ ) will produce a massive of data of  $V/c^2$  for the quadrupole radiation mechanism. The average value of these data will be equal to one.

The right convergent precession  
Fig.41

The right non-convergent precession  
Fig.42

The left convergent precession  
Fig. 43

The left non-convergent precession  
Fig.44

Basing on available data we dare state that the propagation speed of the gravitation radiation is a fundamental magnitude, and its numerical value is equal to about  $9/10^{20}$  cm/sec.

In Fig.41 – 44 there are represented results, which are interesting from the practical point of view. Here the L and R indexes denote left rotation and right rotation of the gyroscope. The dotted curves

duplicate the curves demonstrated in Fig. 39. These curves are represented for comparison. There is a lot material to think about nevertheless one fact is clear, viz the precession of the quadrupole mechanical system, which has a variable angle of precession, is a powerful mechanism of the gravitation radiation that is interesting from the practical point of view.

## § 9. A mathematical model of the quadrupole generator

A mathematical analysis of the experimental device operation was realized independently by O.S. Polyakov, who is a participant of this work. However, the results of the analysis (i.e. machine graphical charts of a central force, which acts on the centre of gravity of the mechanical system during the operation cycle) appeared to be corresponding to those results, which were really observed in the experiment. It should pay attention that the realized analysis was simplified.

**Breath wording of the task:** 1. To calculate the motion of the centre of gravity of the movable part of the balance relatively the unmovable part due to inner forces, which appear during the operation of the force aggregate of the experimental device. (The motion of the centre of gravity of the movable part should be calculated in different dynamic modes).

2. To calculate amplitude characteristics of a response of the indicating part of the balance and to compare them with the propulsion moments, which are really observed.

**The force aggregate description.** The force aggregate of the device is a symmetrical system of four similar gyroscopes, which are articulated with the common support in the suspension brackets. The angle of inclination of the rotation axes of the gyroscopes relatively the axis of the system (of directing screw) is assigned by the position of a thread piece, which slides on the screw along the directing grooves of the aggregate. This thread piece is articulated with the upper articulations of the gyroscopes frames through controlling rods. The geometrical scheme of the force aggregate is represented in Fig.45, where AB is the frame of the gyroscope suspender, BC is the controlling rod, CD is the thread piece. In the process of CD-piece alternate motion the centers of masses of this piece are displaced as well as the centers of masses of the gyroscopes and the rods are done. As the aggregate is symmetrical then the centre of masses of the movable part of the aggregate moves along the axis of the screw. Since that fact in the conditions of the dynamic mode of the aggregate, which is placed on the measuring balance, the mentioned displacement of centers of the masses causes appearance of forces of very mechanical origin.

Fig.45

The geometrical scheme of the force aggregate.

All geometric sizes and masses of elements of the device were accurately measured and the position of the mass centre was defined for every element. For the gyroscope, which is situated in a frame, the radius-vector of the mass centre from the lower articulation  $\bar{r}_2$  has the angle of inclination to the axis of the device of  $\gamma$ . For the rod the radius-vector the mass centre  $\bar{r}_r$  from the point of contact with the thread piece the angle of inclination relatively the axis of the aggregate is denoted as  $\beta$ . Observing the

geometrical scheme it can be seen that  $\beta$  and  $\gamma$  depend only on the position of C articulation of the piece of CD on the axis of the screw  $z$ . Directing the axis downward and accepting A-articulation projection on the axis  $z$  as the computing origin we derive:

$$\cos \gamma = cgp(z) = \frac{z^3 - 102.69 \cdot z + 2\sqrt{z^4 + 118.62 \cdot z^2 + 9249.2361}}{18(z^2 + 4)}, \quad (134)$$

where  $cgp(z) \rightarrow$  cosine of gamma-plus.

$$\cos \beta = cbm(z) = \frac{z^3 + 110.69 \cdot z + 2\sqrt{z^4 + 529.38 \cdot z^2 - 12252.2761}}{27.4(z^2 + 4)}, \quad (135)$$

$cbm(z) \rightarrow$  cosine of beta-minus,  $z$  is a current coordinate of C articulation.

The equation for the general mass centre of the movable part of the aggregate can be written as

$$z_{m.c.}(z) = \frac{\sum m_i z_i}{\sum m_i} = \frac{m_m(z - 0.4) + 4[m_g r_2 cgp(z) + m_r(z - r_r cbm(z))]}{m_m + 4(m_g + m_r)}, \quad (136)$$

where  $m_m$  is mass of the thread piece,

$m_g$  is mass of the gyroscope,

$m_r$  is mass of the rod.

The position of the mass centre of the whole device as a function of  $z$  is

$$z_{m.c.}^{\Sigma} = z_{C_m}(z) = \frac{m_0 z_0 + m_{movable} \cdot z_{m.c.}^{movable}(z)}{m_0 + m_{movable}}, \quad (137)$$

where  $m_0$  is the mass and  $z_0$  is the position of mass centre of the unmovable part of the device.

Now, when we have written in explicit form the dependence of  $z_{m.c.}(t)$ , we can derive the expression for a driving force of  $F_R(t)$ , which change the position of a movable part of the balance relatively an unmovable one. The coordinate  $z$  of the thread piece is uniquely defined by number of turns of a drive screw (step is 2mm).

The dynamics of this rotation was measured in real conditions (Fig.46), which showed that the screw full motion consists of six separate parts:

1. breaking until full stop, which occurs in extreme position,
2. acceleration in opposite direction (reverse),
3. linear path,
4. breaking in the upper extreme position,
5. reverse, accelerated motion,
6. linear path,
1. ...etc.

Fig.46  
Dependence of  $z=f(t)$ .

The function of  $z(t)$  had to be approximated by polynomials, which are listed below, to make it analytical:

- 1) first degree polynomial was used at the linear paths III and VI,
- 2) fourth degree polynomial was used at the acceleration paths II and V,
- 3) fifth degree polynomial was used at the breaking paths I and IV.

The main requirement is continuity of the very function by the coordinate and its first and second derivative in the point of join of solution:

$$\begin{aligned} z_1(t-0) &= z_2(t+0) \\ \left. \frac{dz_1}{dt} \right|_{t-0} &= \left. \frac{dz_2}{dt} \right|_{t+0} \\ \left. \frac{d^2 z_1}{dt^2} \right|_{t-0} &= \left. \frac{d^2 z_2}{dt^2} \right|_{t+0} \end{aligned} \quad (138)$$

The calculation of the coefficients of the polynomials for different periods of one cycle is produced by a program of “inter” (see the appendix). Now let us place the function of  $z(t)$  into the equation (137). Having differentiated it we derive:

$$a_{m.c.} = \frac{d^2 z_{cm}(z(t))}{dt^2} = \frac{d}{dt} \left( \frac{dz}{dt} \cdot \frac{dz_{cm}}{dz} \right), \quad (139)$$

$$F_R = -M \bar{a}_{m.c.} = -M \left[ \frac{d^2 z}{dt^2} \cdot \frac{dz_{cm}}{dz} - \left( \frac{dz}{dt} \right)^2 \frac{d^2 z_{cm}}{dz^2} \right]. \quad (140)$$

Particular programs and subprograms of CYCLE were used to calculate every partial derivative.

Now in the laboratory system of coordinates we direct  $X$  axis upward parallel to the  $z$  axis of the device. The balance does not have other degrees of freedom. We are interested in motion of the movable part of the balance together with the device, which occurs under the action of three forces:

- a) elastic force of the magnetic suspender  $F_{elast.}$ , which is defined for the small oscillations of the balance as

$$F_{elast.} = -kX,$$

- b) outer force relatively  $F_{elast.}$ :

$$F_{outer} = F_R(t),$$

- c) inertia force, which defines final quality of the balance as an oscillating system:

$$F_{inert.} = -\alpha V(t). \quad (141)$$

This task for first two forces can be solved by an analytical way.

Let us write a differential equation for small oscillations of the balance, which occur under the action of an outer force:

$$\frac{d^2 X}{dt^2} + \frac{k}{M} X = \frac{F(t)}{M}. \quad (142)$$

Having denoted  $\sqrt{\frac{k}{M}} = \omega$  (paying attention to the fact that  $\frac{dx}{dt} = V$ ) and introduced a new variable of  $\xi = V + j\omega X$  we rewrite the equation (142) as

$$\frac{d\xi}{dt} - j\omega\xi = \frac{F(t)}{M}. \quad (143)$$

This equation can be easily integrated as

$$\xi = e^{j\omega t} \left[ \int_0^t \frac{F(t)}{M} e^{-j\omega t} dt + \xi_0 \right]. \quad (144)$$

X coordinate becomes

$$X = I_m \left( \frac{[\xi]}{J\omega} \right) = \frac{\cos \omega t}{\omega} \left[ - \int_0^t \frac{F(t)}{M} \cdot \sin \omega t \cdot dt + \omega x_0 \right] + \frac{\sin \omega t}{\omega} \left[ \int_0^t \frac{F(t)}{M} \cos \omega t \cdot dt + V_0 \right]. \quad (145a)$$

The speed is

$$V = R_e [\xi] = \cos \omega t \left[ \int_0^t \frac{F(t)}{M} \cdot \cos \omega t \cdot dt + V_0 \right] + \sin \omega t \left[ \int_0^t \frac{F(t)}{M} \cdot \sin \omega t \cdot dt - \omega X_0 \right]. \quad (145b)$$

Hence, we know the motion of the balance without taking the inertia force into account.

Let introduce the inertia force, assigning the initial conditions of  $X_0$ ,  $V_0$ , and the interval of  $\Delta t$ , which should be small enough to  $F_{inert.} \cong const$  in it. Then:

$$F_{inert.} = -\alpha V(t) = -\frac{\omega M}{\pi Q} \cdot V(t), \quad (146)$$

where Q is the quality of the balance as a mechanical oscillating circuit.

In this interval there is

$$F(t) = F_R(t) - \alpha V(t_0). \quad (147)$$

Then the coordinate X and the speed V in the moment of  $t_0 + \Delta t$  are calculated. These values are used as basic values for the next step etc. the powerful force  $F_R(t)$ , which graphical chart is demonstrated in Fig.45, produces auto-oscillations of the balance. These auto-oscillations mask a useful signal as it is shown in Fig.48.

A filter of damped sine is used to extract the useful signal as it is demonstrated in Fig.49. This filter rejects harmonic constituents of the useful signals. Nevertheless it shows amplitude and phase changes of the system in qualitatively correct way. As it is demonstrated in Fig.49 the input signal  $U_0$  is

divided into positive component and negative component  $(U_+, U_-)$ . Both components come to a particular charge circuit RC, and the time constant of the circuit is a little less than the time constant of the balance:

$$\frac{1}{RC} = k \frac{\omega}{2\pi Q}. \quad (148)$$

Fig.47  
The dependence of  $F_R(t) = f(t)$

Fig.48  
Masking effect of the useful signal by auto-oscillations of the balance

Fig.49  
The filter of damped sine

As it has been defined by the experiment  $k_{opt} \cong 2.3$ . This filter is easy to be approximated by a program:

$$\begin{aligned} U_+^c &= U_0 \text{ at } U_0 \geq U_+^c \\ U_+^c &= U_+^{c \max} \exp\left(-\frac{t}{RC}\right) \text{ at } U_c < U_+^c \\ U_-^c &= U_0 \text{ at } U_0 \leq U_-^c \\ U_-^c &= U_-^{c \min} \exp\left(-\frac{t}{R_c}\right) \text{ at } U_0 > U_-^c \end{aligned} \quad (149)$$

The output signal is

$$U_1 = U_-^c + U_+^c \quad (150)$$

Variants of the output signal are represented in Fig.50 and 51.

Having mathematically modeled the filter and introduced it into the program of CYCLE we can form graphical charts. These graphical charts are analogous to the signals, which were really observed in the process of experimental investigation of the force aggregate.

Now let us revise that the calculated force of  $F_R(t)$  displaces the balance from the equilibrium position. It is obtained only from the condition of alternate motion of the thread piece along Z axis. However the force aggregate allows a gyroscope precession, which has a variable angle (both of rotating gyroscopes and of unmovable ones, i.e. at  $\omega_0 = 0$ ).

Fig.50

Fig.51  
“Filtered” signal

Thus, centrifugal forces act in the system as well as gyroscopic central forces, which were unknown earlier. These forces are applied to the centre of gravity of the mechanical system. As it is known, the centrifugal forces, which rotate around Z axis, do not have components along Z axis. Now we have achieved the culmination point of our analysis. As it is known, the orthodox classical mechanics does not allow central forces exist as if they break the law of momentum conservation. Hence, the classical mechanics does not admit that energy directed radiation is possible at non-relativistic curvilinear motion of any mass of non-cosmic size.

This paragraph of this work is devoted to overthrow of that unfounded tenet. Non-classical forces, which were formulated by S.M. Polyakov, were introduced into the worked-out program:

- a) a gyroscope rotation effect with a variable radius,
- b) a precession effect of the system of gyroscopes with a precession variable angle.

The a) case is realized by simultaneous superposition of rotation of a system, which has angular velocity  $\Omega$  relatively Z vertical axis, on the thread piece independent cyclic displacement along Z axis.

The b) case is automatically derived from a) in the case of adding the gyroscopes proper rotation ( $\omega_0 \pm$ ).

The motion is cyclic as before.  $\Omega = \Omega(t)$  acts for one half of the period of  $Z(t)$  function, i.e. the system does translational-rotational motion, during the other half of the period the system makes alternate motion into the initial position ( $\Omega = 0$ ).

As it can be seen from the geometrical scheme, which is demonstrated in Fig.45, in the case of the thread piece motion the radiuses of rotation of mass centers of the gyroscopes and the rods relatively Z axis.

The radius of general rotation of mass center of the gyroscope and the rod becomes

$$r_{rot} = \frac{m_r (4.7 + r_r \cdot \sin \beta) + m_{gyr} (6.7 + r_{gyr} \cdot \sin \gamma)}{m_r + m_{gyr}}. \quad (151)$$

The additional central force is

$$F_{rot.add.} = \frac{V}{c^2} W = \frac{V}{c^2} 2k\gamma_0 \Omega_{\mp}^{3/2} \cdot \frac{M_r^2}{r_r^2} \left( \frac{dr_r}{dt} \right)^{\pm} \cdot k_{pr}, \quad (152)$$

where  $\frac{V}{c^2} = 1$ ;  $2k = 1$ ;  $\gamma_0 = \frac{1}{137}$ ;  $k_{pr} = 0.1$ .

In turn

$$\frac{dr_r}{dt} = \frac{1}{m_r} \left[ m_r \cdot r_r \cdot \frac{d}{dZ} \sqrt{1 - cbm^2(Z)} + m_{gyr} \cdot r_r \cdot \frac{d}{dZ} \sqrt{1 - cgp^2(Z)} \cdot \frac{dZ}{dt} \right], \quad (153)$$

where  $m_r = 4(m_r + m_{gyr})$ .

Fig.52

The dependence of  $\Omega = f(t), L = f(t)$ .

If the function of  $Z(t)$  increases at the active path of  $\Omega \neq 0$  then  $\frac{dr_r}{dt} < 0$  and the mode is named as “convergent fan”. If  $Z(t)$  decreases then  $\frac{dr_r}{dt} > 0$  and the mode is named as “non-convergent fan”.

A real graphical chart of  $\Omega$  function is represented in Fig.52 and approximated by the following functions:

$$\Omega(t) = \begin{cases} \frac{\Omega_{\max}}{\exp\left(\frac{t_1 - t}{\Delta_1} + 2\right) + 1} & \left. \begin{array}{l} t_{pr} \\ t_1 \end{array} \right\} \text{at the path of switching-acceleration} \\ \frac{\Omega_{\max}}{\exp\left(\frac{t_1 - t}{\Delta_1} + 2\right) + 1} & \left. \begin{array}{l} t_3 \\ t_{pr} \end{array} \right\} \text{at the path of breaking-stop} \end{cases}$$

$\Delta_1$  is a parameter of  $\Omega$  increase at the electric engine switching on,  
 $\Delta_2$  is a parameter of  $\Omega$  decrease at the electric engine switching off.

The function of  $L(t)$  is approximated in the same way.

If the gyroscopes are simultaneously switched on at the force (152) then one more central force begins to act, i.e.

$$F_{add}^{gyr} = \frac{V}{c^2} W = \frac{V}{c^2} \cdot L_{\pm}^{gyr} \cdot \Omega_{\pm} \cdot \cos \gamma \left( \frac{d\gamma}{dt} \right)^{\pm} \cdot k_g, \quad (155)$$

where  $\frac{V}{c^2} = 1$ ;  $k_g = 10^{-3}$ ;  $\gamma = \text{Arc cos } cgp(z)$ ;

$$\frac{d\gamma}{dt} = - \frac{dz}{dt} \cdot \frac{dcgp(z)}{dz} \cdot \frac{1}{\sqrt{1 - cgp^2(z)}}. \quad (156)$$

the whole program is represented in the appendix 1.

The results of the calculations of  $F_{dyn} = F(t)$  are demonstrated in Fig. 53 – 61.

Fig.53 shows the simplest case, which is possible to be described by the classical mechanics, viz “swinging blanks”.

From the point of view of the mechanics the response of the balance is defined by final values of the function of  $F(t)$  in the points of  $Z_{\max}(t)$  and  $Z_{\min}(t)$  that is independent of the way of motion between these points.

Thus the “classical calculation” must be finished by the graphical chart (Fig.53)!

In Fig.53 the dotted line demonstrates an equilibrium position of the balance, when it is in the rest state (0 of rest), and the firm line demonstrates the function of  $F(t)$  during one cycle of the force aggregate action. Since the acceleration of propulsion produces asymmetry in the vertical translational motion of the common center of masses then in the dynamic mode the equilibrium state moves into the area, which is represented by the firm line (0 of dynamics).

In fig.54 the calculated dependence of  $F(t)$  is represented for the cyclic precession of the unmovable gyroscopes (the precession of the blanks). For comparison the effect of “swinging blanks”, which equilibrium state is a dynamic zero for the effect of the precession of the blanks. As it is evident from the figure the precession of the blanks, which is left, non-convergent, produces a positive propulsion effect, and the right, non-convergent precession makes a negative propulsion effect. In spite of the effects are not expected by the classical mechanics they are observed in a real experiment.

In Fig.55 analogous results, which were obtained for the convergent precession of the blanks, are demonstrated. Here in accordance with our force equations the propulsion effect changes its sign.

Simultaneously with the sign changing there is  $\frac{dr}{dt}$  for every direction of the angular speed of  $\Omega$  precession. It is interesting that the additional force effect for the left convergent precession is equal to zero during the cycle of action of the device.

In Fig.56 there are the results of calculation of the action of the complex of forces at the precession of the system of rotating gyroscopes with a variable precession angle. Here the dependence of  $\sum F = f(t)$  describes the right convergent precession of the gyroscopes for both the right and left direction of the gyroscopes proper rotation. The effect of the precession of the blanks, which equilibrium state is a dynamic zero for the precession of the gyroscopes in this case, is represented by the firm line. Real oscillograms are demonstrated nearby for comparison of the calculated curves with the real dotted lines.

Calculation

Experiment

Fig.53

Calculation of the function of  $F = F(t)$ . Swinging blanks

The right non-convergent precession of the “blanks”

The left non-convergent precession of the “blanks”

Swinging of the “blanks”

Fig.54

Calculation of the function of  $F(t)$ , precession of the blanks

The right convergent precession of the “blanks”

The left convergent precession of the “blanks”

Swinging of the “blanks”

Fig.55  
Calculation of the function of  $F(t)$ , the precession of the blanks

In Fig.57 there are demonstrated the results obtained for the left convergent precession of the gyroscopes. Here the experiment badly correlates with the calculation, especially for the left rotation of the gyroscopes. Probably, it is connected with the fact that the effect of the gyroscopes swinging, which influences on the general case in a certain way, was not included into the program:

$$\Delta F = \frac{V}{c^2} \frac{8\gamma_0}{r^5 \omega_0^{1/2}} L(t) \frac{dL}{dt}. \quad (157)$$

The calculation looks like the experiment made for the right rotation.

In Fig.58 the results of calculation of the force function for the right non-convergent precession (a) and for the left non-convergent precession (b) are represented for the both directions of the gyroscopes rotation.

The right convergent  
precession of the “blanks”

experiment

Experiment

The gyroscopes are “to the left”

The gyroscopes are “to the right”

Fig.56  
Calculation of the function of  $\sum F = f(t)$  for the precession of the gyroscopes

The results of the calculation qualitatively agree with the results of the experiment that demonstrates that the dynamic effects are real and caused by the action of some mechanical forces, which were unknown and undescribed before. These forces accompany the rotation of the classical gyroscope with a variable radius as well as the precession of the gyroscopic symmetrical system with a variable precession angle.

**Thus the same equations, which were used to calculate a propagation speed of an unknown radiation due to the recoil momentum, were used to solve the classical problem of investigation of the centre of masses of a mechanical oscillation system. These equations allowed calculate the recoil moments of the mechanical system, which are analogous to the moments, which are really observed at the screen of an oscillograph.**

Thus our equations were directly and indirectly tested in contrast to unfounded assertions of our opponents. Obviously, these materials are of practical interest. Nevertheless, the issues of practical

application will be discussed in a separate work. (Those people, who want to get the program, can appeal to the author).

Hence, let us make conclusions of this chapter.

1. It has been theoretically predicted that in a non-linear mechanical axially symmetric (i.e. non-eccentric) system the appearance of central forces, which are non-compensated during the cycle of action. These forces make the centre of gravity of the mechanical system **directly move**, hence, the whole system is made to move as well. This fact was proved by an experiment, which conditions were analyzed.

Unsupported motion is possible.

2. The very fact of the strong forces existence can be explained by only one way, i.e. a non-linear mechanical system radiates a new type of energy, which is unknown for the modern science.
3. The approximate experimental evaluation of the propagation speed of this radiation produces the following values:
  - a) there is  $10^8 \div 10^9 C$  for a dipole radiation
  - b) there is  $3 \cdot 10^{10} C = 9 \cdot 10^{20} \text{ cm/sec}$  for a quadrupole radiation.

The last value is the second fundamental velocity of matter propagation in the world.

4. We have a copyright and must be the first to detect this radiation.

a) The right non-convergent Experiment  
Precession of the “blanks”

The gyroscopes are “to the left”

Experiment

The gyroscopes are “to the right”

c) The left non-convergent  
Precession of the “blanks”

The gyroscopes are “to the right”

Experiment

The gyroscopes are “to the left”

Fig. 58

Calculation of the function of  $\sum F = f(t)$  for the precession of the gyroscopes

## § 10. The issues of practical application of the obtained results

In this moment we have impulse thrust of  $F \cong 1 \text{ kg}$  at the summarized mass of the gyroscopes of  $m_0 = \sum m_1 = 6.4 \text{ kg}$ , the rotation frequency of the gyroscopes of  $\omega_0 \cong 2\pi \cdot 50 \text{ c}^{-1}$ , the precession

frequency of  $\Omega \cong 1.5$  rad/sec, and the general mass of  $M_{\Sigma} \cong 32$  kg. Let us observe the potentials of the construction optimization. The working equation is:

$$F = \frac{V}{c^2} \cdot \frac{4\gamma_0 m_0}{r^3 \omega^{1/2}} \cdot L \cdot \Omega \cdot \cos \varphi \cdot \frac{d\varphi}{dt}. \quad (158)$$

$$\text{At } \frac{V}{c^2} = 1; \frac{8k\gamma_0}{\omega^{1/2}} \text{ const}; \Omega = \text{const}; \omega = \text{const}; \frac{d\varphi}{dt} = \text{const}; \cos \varphi = \max = 1.$$

It can be represented as

$$F = \text{const} \cdot \frac{m_0 L}{r^3}, \quad (159)$$

for a spherical gyroscope  $m_0 \approx r^3$ .

Hence the expression (159) finally becomes

$$F = c \cdot m^{5/3}. \quad (160)$$

Mass of the engine  $M_{\Sigma}$  consists of the following components:

$$M_{0\Sigma} = m_0 + M_{AD}, \quad (161)$$

where  $m_0$  is the mass of the gyroscopes,

$M_{AD}$  is the mass of an armature and a power drive.

Supposing  $M_{AD}$  to be proportionate to the power of the engine, i.e.  $M_{AD} \approx m^{5/3}$ , we observe its minimal value:

$$M_{AD} = m_x^{5/3}, \quad (162)$$

where  $m_x$  is an unknown mass of the gyroscope.

Hence

$$M_{0\Sigma} = m_x + m_x^{5/3} \quad (163)$$

is the minimal mass of the engine, which is normalized to the mass of a gyroscope:

$$M_{\Sigma} = \frac{M_{0\Sigma}}{m_x} = 1 + m_x^{2/3}. \quad (164)$$

The relation of

$$\frac{F}{M_{\Sigma}} = \frac{m^{5/3}}{1 + m^{2/3}} \quad (165)$$

is a specific impulse to the unit of the mass of the engine, and it can be identified as an acceleration in  $g$  units, i.e. units of the acceleration of the terrestrial gravity. Now let us view real potentialities to increase the propulsion  $F$  within the existent construction.

A graphical chart of the function of  $F_1 = f\left(\frac{m}{m_0}\right)$  is demonstrated in Fig.59. In this figure the dependence of

$$\frac{F}{M_\Sigma} = \frac{m_x^{5/3}}{1 + m_x^{2/3}}$$

is also represented.

Fig.59

The dependence of absolute propulsion of  $F(x) = f\left(\frac{m_x}{m_0}\right)$  and relative propulsion of  $\frac{F_x}{M_\Sigma} = f\left(\frac{m_x}{m_0}\right)$  on the mass of the gyroscopes.

Comparing the graphical charts it is evident that  $\frac{F}{M_\Sigma} = 2$ , and  $F \cong 170$  kg at  $m = 3m_0$  and the proper weight of about 90 kg.

Thus, the problem of the priority of “practical result or trust” should be solved in favour of the trust.

We have touched upon the subject of practical application, and the issue should be regarded as a very important one because force gyroscopes of 30-60000 turns/minute are a very serious thing.

## Chapter 2

### Experimental Proof of Regularity of Connection of Magnetism with Gravitation as Consequence of Electron Microstructural model

The existence of this connection was suspected in the beginning of the XX century since A. Einstein’s GR had appeared. The point is that at certain limitation conditions and some simplification the equations of GR comes to Maxwell’s system of equations that produces an illusion of simplicity of the problem of the connection of the magnetism with the gravitation. Even a term of electromagnetic-

gravitational analogy has appeared. The majority of theoretical investigations were made in this direction, for example [14]. The investigations gently and visually show that all laboratory attempts to observe strong gravitation effects are doomed to fail!

Following this path no author has extracted the essence of the connection of the magnetism with the gravitation, penetrated into a mechanism of transformation of one energy type into another one, and predicted new observable laboratory effects. As a result the investigators began to pay their whole attention to the cosmic cataclysms as the only source of powerful gravitation effects. The first attempt to state a quantitative connection between the magnetism and the gravitation or rather a connection between a magnetic field and a gravitation one was made by E. Teller [15]. He identified the gravitation field with a centrifugal acceleration field. For a rotating charged body he obtained the following equation:

$$\bar{H} = \frac{e}{c^3} [\bar{g} \times \bar{\omega}], \quad (167)$$

where  $\bar{H}$  is an intensity of the magnetic field,  
 $e$  is a charge of electrically polarized rotating mass,  
 $g$  is the centrifugal acceleration,  
 $\omega$  is an angular speed of the body rotation,  
 $c$  is the light speed in a free space.

From the point of view of an experiment the equation (167) predicts a laboratory effect, which is similar to Barnett's effect and no more. Our approach, which is based on physical modeling of a microstructure of a rest electron that has been observed in the part I of this work, has appeared to be more fruitful. It follows our model that the equivalent energy of an electron rest mass is a magnetostatic energy and is defined by a product of the electron proper magnetic momentum and its proper magnetic field. The gravitation energy of a rest electron 137 times exceeds its magnetostatic energy. Supposing that proportions between interrelated values are safe at a transition from the microworld to the macroworld we have obtained a single-valued connection between the magnetic energy and the gravitation energy of a macroscopic magnetized ferromagnetic:

$$W = \frac{B \cdot H \cdot V}{\alpha}. \quad (87)$$

Thus in our opinion there is no direct connection between the magnetic field and the gravitation field. However, there is a regular connection between the magnetic energy and the gravitational one that is realized on a level of the microworld of elementary particles. Therefore indeed Maxwell's electrodynamics has not worked. More over, our electron model demonstrates that an electron gravitation radius is equal to a half of its classical value, i.e. about  $1.4 \cdot 10^{-13}$  cm.

Having these data and the equation (87) we can define a scalar gravitation potential of a magnetized ferromagnetic, i.e. its gravitation field. As it is known, on the surface of the gravitation radius of any object (as a black hole or an electron) the scalar gravitation potential is equal to  $c^2$ , where  $c$  is the light speed in the free space. We suppose that one element of a crystal lattice of the ferromagnetic contains just one electron of exchange interaction. Then knowing that, according to definition, the scalar gravitation potential decreases as well as the distance from a gravitating centre does, we can define an average value of the scalar potential due to the element of the crystal lattice:

$$\bar{\varphi} = c^2 \cdot \frac{r_0}{2r_p} = c^2 \frac{1.4 \cdot 10^{-13}}{10^{-8}} = 1.4 \cdot 10^{-5} c^2 = \Phi_s, \quad (168)$$

where  $r_p \approx 10^{-8}$  cm is a constant of the lattice.

The value, which is approximately defined by the expression (168), is the maximal value of the scalar gravitation potential for the whole ferromagnetic, which is magnetized up to saturation. Then the scalar potential for an arbitrary magnetized ferromagnetic is

$$\Phi = \Phi_s \frac{(B \cdot H)}{(B \cdot H)_s} = 1.4 \cdot 10^{-5} \cdot c^2 \frac{(B \cdot H)}{(B \cdot H)_s}, \quad (169)$$

where  $S$  index means a magnetization saturation point. It is evident that the magnetization of the ferromagnetic by a non-homogeneous magnetic field produces a gradient of the scalar gravitation potential, which appears simultaneously with a magnetization gradient. The gradient of the scalar gravitation potential is equivalent to the acceleration of the terrestrial gravity, i.e.

$$\text{grad}\Phi = \frac{1.4 \cdot 10^{-5} c^2}{(BH)_s} \cdot \text{grad}(BH). \quad (170)$$

Let us numerically evaluate this acceleration in g units, i.e. in the units of the acceleration of the terrestrial gravity. According to the real parameters of the ferromagnetic, which was used during our experiments, there is  $(BH)_s = 1.6 \cdot 10^8$  Erg/cm<sup>3</sup> and  $\text{grad}(BH) = 6 \cdot 10^7$  Erg/cm<sup>4</sup>

$$\text{grad}\Phi = 1.4 \cdot 10^{-5} \cdot 9 \cdot 10^{20} \frac{6 \cdot 10^7}{1.6 \cdot 10^8} \approx 4.72 \cdot 10^{12} g. \quad (171)$$

The numerical evaluation demonstrates the gravitation fields of cosmic quantities to be around us. Since our issues are very interesting from the point of view of practice and science then it is useful to test them. Are they experimentally proved? What are those experiments? What new effects can be expected during laboratory investigations? These problems are covered in the following paragraphs of this book.

## § 1. Gravitational interpretation of a magnetostriction

An effect of change of linear dimensions and capacity of a ferromagnetic during magnetization was disclosed by J.P. Joule in 1842. Magnetostriction is widely applied in modern technics nevertheless the Physical Encyclopedia [16] contains a declaration: “Longitudinal magnetostriction and transversal magnetostriction of the majority of ferrites are negative; the cause of the phenomenon is unknown”.

What do we know about this effect in 150 years after its discovery?

1. Linear magnetostriction can be positive as well as negative. Volume magnetostriction is always negative.
2. The magnetostriction is an even effect, which is independent of a direction of an acting magnetic field.
3. The magnetostriction has hysteresis as well as the magnetization does.
4. The modern theory of magnetism can calculate only the linear magnetostriction for crystals of cubic symmetry that can be only in the area of para-processes and only in the presence of two constants of magnetostriction anisotropy, which must be experimentally defined beforehand. Obviously, wide application does not mean fundamental understanding.

The first calculation of the magnetostriction was made in 1928 by N.S. Akulov [11]. The magnetostriction in the area of para-processes was defined by the expression on

$$\lambda_s = \frac{\Delta l}{l} = \lambda_1 \left( S_1^2 \beta_1^2 + S_2^2 \beta_2^2 + S_3^2 \beta_3^2 - \frac{1}{3} \right) + 2\lambda_2 (S_1 S_2 \beta_1 \beta_2 - S_2 S_3 \beta_2 \beta_3 + S_1 S_3 \beta_1 \beta_3), \quad (172)$$

where  $S_1$  is direction cosines of a magnetization vector

$\beta_1$  is direction cosines of the magnetostriction direction,

$\lambda_1, \lambda_2$  are the magnetostriction constants.

The listed facts make the idea of defining the magnetostriction as a gravitation effect very tempting.

Hence, let us try to derive a proper equation of magnetostriction and compare it with known experimental results. Let us revise that the product of  $(BH)$  is a density of the magnetic energy  $E_M$ , according to definition. It can be written as

$$BH = \frac{E_M}{V} = \frac{B^2}{\mu}. \quad (173)$$

At periodical change of the outer magnetic field  $H$  it follows the equation (173) that

$$\frac{1}{V} \frac{\partial E_M}{\partial H} - \frac{E_M}{V^2} \frac{\partial V}{\partial H} = \frac{2B}{\mu} \frac{\partial B}{\partial H} - \frac{B^2}{\mu^2} \frac{\partial \mu}{\partial H}. \quad (174)$$

the equation (174) simultaneously describes two process:

$$\left. \begin{aligned} \frac{1}{V} \frac{\partial E_M}{\partial H} &= \frac{2B}{\mu} \frac{\partial B}{\partial H} \\ \frac{E_M}{V^2} \frac{\partial V}{\partial H} &= \frac{B^2}{\mu^2} \frac{\partial \mu}{\partial H} \end{aligned} \right\}$$

change of the density of the magnetic energy

the proper magnetostriction. (175)

In real experiments on the magnetostriction the outer magnetic field, which is generated by magnetizing coils, is homogeneous. Therefore, probably, transversal constituents of the magnetic field as well as transversal constituents of the magnetization can be neglected.

Since our calculation is approximate then we neglect transversal constituents of the magnetostriction in spite of we do not have enough reasons to do it.

Then the equation of the magnetostriction becomes

$$\frac{1}{V} \frac{\partial V}{\partial H} = \frac{B^2}{\mu^2 (BH)} \frac{\partial \mu}{\partial H} = \frac{1}{l} \frac{\partial l}{\partial H} = \lambda. \quad (176)$$

Now let us pay attention to the fact that redefinition of the magnetostriction has occurred in the process of our analysis. The equation of  $\lambda = \frac{\Delta l}{l}$  has turned into  $\lambda = \frac{1}{l} \frac{\partial l}{\partial H}$  that is far not the same thing.

However, if we reflect on the problem then we can realize that the value of  $\frac{\partial l}{\partial H}$  is measured in the experiments on the magnetostriction! What is the connection with the gravitation? The answer is following. We can define a constant of the magnetostriction in the magnetization saturation point as

$$\sigma_s = \frac{\alpha \cdot k}{(BH)_s}, \quad (177)$$

where  $\frac{(BH)_s}{\alpha}$  is density of the gravitation energy in the magnetization saturation point,

$k$  is a parameter of participation of the gravitation field of magnetic cores of ferromagnetic ions in the effect of the magnetostriction.

Hence, a final variant of the working equation of the magnetostriction is

$$\lambda = \frac{1}{l} \frac{\partial l}{\partial H} = \frac{\alpha \cdot k}{(BH)_s} H^2 \frac{\partial \mu}{\partial H}. \quad (178)$$

Thus, the gravitation comes to the equation of the magnetostriction twice, i.e. as the constant of the magnetostriction and as the parameter of participation of the magnetic cores.

Now let observe qualitative correspondence of the equation (178) to the real peculiarities of the phenomenon of the magnetostriction, which are listed above.

1. A sign of the magnetostriction is defined by a sign of  $\frac{\partial \mu}{\partial H}$ , i.e. by a curve of technical magnetization, which has been measured in the direction of the calculated component of the linear magnetostriction.
2. A graphical sum of three linear components of the magnetostriction, which have been calculated due to three basic axes of anisotropy of the pattern form, is always negative, and its numerical value is close to the volume magnetostriction value.
3. The magnetostriction is an even effect as the squared magnetic field value comes into the equation.

4. Magnetic penetrability  $\mu$  is a hysteresis value hence the differential penetrability of  $\frac{\partial\mu}{\partial H}$  is a hysteresis value hence the very magnetostriction is a hysteresis value as well.

Thus, from the qualitative point of view now everything agrees. We need experimental dependences of  $B=f(H)$  and of  $\lambda = f(H)$  for the same pattern to test the agreement of the theory with the experiment.

Unfortunately, we did not have such an opportunity therefore we had to use only the dependence of  $B=f(H)$  for Armko iron and for technically pure nickel and to compare the calculation results with reliable experimental data according to literature sources [17].

### **The experimental results**

In Fig.60 the results for nickel are demonstrated, i.e. an experimental curve of the technical magnetization, an experimental curve of the magnetostriction of  $B=f(H)$  and a calculation curve of the magnetostriction, where the parameter is  $K=6.5$ . The experiment quite satisfactorily agrees with the theory. In Fig.61 the analogical results obtained for Armko iron are represented. Here the agreement of the experiment with the calculation is very satisfactory ( $K=1$ ).

Thus, the experiment has proved validity of our approach of the problem of the magnetostriction. Hence it has proved gravitational essence of this mechanism, i.e. the compression of matter in its proper magnetic field. This fact should be added to the Physical encyclopedia to the part of "Magnetostriction".

Nickel

Fig.60

The dependence of the magnetostriction of the technically pure nickel on the value of the applied magnetic field

Armko

Fig.61

The dependence of the magnetostriction of the Armko iron on the value of the applied magnetic field

## **§ 2. Magnetostriction curvature of an optic beam**

This effect as well as the very magnetostriction is a gravitational one in spite of it is not that light beam curvature, which was predicted by A. Einstein's General Relativity.

In general the light beam curvature in a medium of a variable coefficient was theoretically described as a hypothesis in a course of physics by Frish and Timofeeva in 50<sup>th</sup> [18]. However, a magnetostriction

variant of the effect was predicted and experimentally discovered by the author of this work on 25 of May in 1975 [19]. It should be noted that it firstly was interpreted by the author as a gravitation effect only.

Following gravioptic experiments and decoding of the magnetostriction mechanism provided the author with a necessary material for clarification of this issue.

Thus, let us observe some capacity of an optically transparent ferromagnetic, which is placed into the non-homogeneous magnetic field with a specified gradient. The magnetic field gradient produces the magnetization gradient in the medium that causes the magnetostriction gradient in the ferromagnetic, i.e. the gradient of intrinsic pressure in the medium. The gradient of the intrinsic pressure immediately causes a gradient of the medium refraction coefficient. If an optic beam comes through the medium normally to a vector of the gradient of the refraction coefficient then it deviates by an angle, which is defined by the expression of

$$\Theta = \frac{l}{n_0} \text{grad } n, \quad (179)$$

where  $n_0$  is an undisturbed coefficient of the medium refraction,  
 $l$  is the beam medium path.

In the work [20] an increment of the refraction coefficient as of the function of the intrinsic pressure in the medium is defined by the expression of

$$\Delta n = q \frac{(n_0^2 - 1)(n_0^2 + 2)}{6n_0} \Delta P_s, \quad (180)$$

where  $q$  is compressibility of the medium,  
 $\Delta P_s$  is the pressure increment at adiabatic compression.

For the adiabatic process there is

$$q = - \frac{c_p}{c_v} \frac{1}{V} \left( \frac{\Delta v}{\Delta P} \right)_s \quad (181)$$

where  $c_p$  is isobaric heat capacity,  
 $c_v$  is isochoric heat capacity,  
 $v$  is the initial volume of matter.

Placing the expression (181) into the expression (180) we obtain

$$\Delta n = - \frac{(n_0^2 - n_0^2)(n_0^2 + 2)}{6n_0} \frac{c_p}{c_v} \frac{\Delta v}{v}. \quad (182)$$

It is evident that in this case  $\frac{\Delta v}{v}$  is nothing but the volume magnetostriction, which can be represented as

$$\frac{1}{v} \frac{\partial v}{\partial H} \cong \frac{\alpha k}{(BH)_s} H^2 \frac{\partial \mu}{\partial H}. \quad (183)$$

Turning from the refraction coefficient in the equation (182) to a magnetic field derivative and using the expression (183) we obtain

$$\frac{\partial n}{\partial H} = - \frac{(n_0^2 - 1)(n_0^2 + 2)}{6n_0} \cdot \frac{c_P}{c_V} \cdot \frac{\alpha k}{(BH)_s} H^2 \frac{\partial \mu}{\partial H}. \quad (184)$$

Hence the final variant of the gradient of the refraction coefficient is

$$grad_x n = \frac{\partial n}{\partial H} \frac{\partial H}{\partial X} = + \left[ \frac{(n_0^2 - 1)(n_0^2 + 2)}{6n_0} \cdot \frac{c_P}{c_V} \cdot \frac{\alpha k}{(BH)_s} H^2 \right] \frac{\partial \mu}{\partial H} \frac{\partial H}{\partial X} = [ ] grad_x \mu. \quad (185)$$

$\frac{c_P}{c_V} = 1.13$  for a grout of manganese chloride, which was used in the experiment, and the undisturbed refraction coefficient  $n_0 = 1.33$  at frequency of a helium-neon laser, which was used in the experiment. After all substitutions and reductions the equation (179) finally becomes

$$\Theta = +0.3l \frac{\alpha k}{(BH)_s} H^2 grad \mu \quad (186)$$

(‘+’ sign in the equations (185) and (186) is caused by the fact that the volume magnetostriction is always negative).

Electromagnet

Working dish

Fig.62

Scheme of the experiment on the curvature of the optic beam in the non-homogeneously magnetized ferromagnetic (the solution is  $MnCl_2 \times 4H_2O$ ).

solution of  $MnCl_2$

Fig.63

The dependence of optic transparent of the grout of manganese chloride on the wave length (the results were obtained by means of a spectrophotometer of CΦ-10)

The scheme of the experiment on the beam curvature in a non-homogeneously magnetized ferromagnetic is represented in Fig.62.

### Choosing of material for the magnetogravioptic investigations

We used a fat water solution of manganese chloride ( $MnCl_2 \times 4H_2O$ ) with the undisturbed refraction coefficient of  $n_0 = 1.332$  as a working matter. The material is relatively accessible, optically transparent but time unstable. Unfortunately, we did not succeed in procuring of other materials.

Optic transparence of the manganese chloride solution, which was measured by an automatic spectrophotometer of CΦ-10 at a 40-millimeter working dish, is demonstrated in Fig.63. The graphical chart shows that the optic transparence comes to 98-99% at the frequency of He-Ne-laser (OKΓ-13).

The results of the magnetic measurements of the solution is represented in Fig.64, where there are the dependences of  $B=f(H)$ ,  $(B - H)=f(H)$  and  $\mu = f(H)$ . As it is seen from the dependence of  $(B - H)=f(H)$  magnetic saturation of the solution occurs at the outer magnetic field of  $H \cong 12000E$ . the dependence of  $B=f(H)$  shows that the solution is a weak ferromagnetic. However it is a ferromagnetic and no more! The graphical charts in Fig.64 are the basement for the following calculations and used in an analysis of the experimental results.

solution of  $MnCl_2$

solution of  $MnCl_2$

Fig.64

An experimental dependence of  $B=f(H)$  for the manganese chloride solution (according to the data of Table 1). The dependences of  $(B - H)=f(H)$  and  $\mu = f(H)$  has been calculated.

### Parameters of a magnetic gap

The non-homogeneous magnetic field, which was used in the optic experiments, was generated by the system of two wedge-shaped pole tips. The angle between the wedge generators is equal to  $90^\circ$ , and the distance between the tops is equal to 10 mm. The magnetic gap was fixed by a special arbor.

Experimental results of measurement of the non-homogeneity of the magnetic field in this gap are represented in Fig.65. According the measuring results represented in Fig.64 and Fig.65 the dependences of  $grad_z B = f(H)$  and  $grad_z (BH) = f(H)$  were calculated. They are demonstrated in Fig.66 and are the basement for all the following calculations.

Fig.65

The experimental dependence of  $grad_z H = f(H)$  in the real magnetic gap

solution of  $MnCl_2$

$grad_z B$  (calculation)

$grad_z (BH)$  (calculation)

Fig.66

The dependences of  $grad_z B = f(H)$  and of  $grad_z (BH) = f(H)$ , which have been calculated due to the graphical charts demonstrated in Fig.66 and 67.

### The experiment method

As it is schematically shown in Fig.62 the laser beam came through the working dish, which was placed into the non-homogeneous magnetic field of the wedge-shaped pole tips of the electromagnet. The dish was parallel to the flat of the maximal magnetic field (at 2.5-3-milimeter distance from it). the working dish is 80-milimeter-long. At 2-meter distance from an output window of the dish the beam was projected onto a screen, which fixed a displacement of a centre of a light spot, which occurred at change of the magnetic field.

The results of the measurements are represented in Fig.67 as dependences of  $\Theta_E = f(H)$ ,  $\Theta_{dr} = f(H)$ , and  $\Theta_M = f(H)$ , where  $\Theta_E$  is an experimental value of a curvature angle measured in angular minutes,  $\Theta_M$  is a theoretical value of the curvature magnetostriction effect (in minutes),  $\Theta_{dr}$  is a difference between the theoretical value and the experimental value. This difference defines the influence of an effect of magnetic ions drift onto the area of the maximal value of the magnetic field.

Due to the results of comparison of the experiment with the calculation a real dependence of the gradient of the refraction coefficient on the magnetic field value was calculated. The gradient of the refraction coefficient is caused by the magnetic ions drift. This dependence of  $grad_z H = f(H)$  is represented in Fig.67 by the dotted line.

As it is evident from the table of the calculation data and from Fig.67 the effect of the beam curvature is caused by the magnetic ions drift up to the field of 6000 Oersted order. The magnetic ions drift comes to its saturation at about 8000 Oersted. In the area of higher magnetic fields the subsequent increase of the curvature angle occurs due to the magnetostriction component of the refraction coefficient increment.

From our point of view a fundamental result of this investigation is the very fact of disclosing of the effect, which was predicted in 1975.

Fig.67

Effect of the curvature of the light beam in the solution of  $MnCl_2$ ,  $\Theta_{dr} = f(H)$  is the beam curvature occurring due to the magnetic ions drift;  $\Theta_M$  is the beam magnetostriction curvature (calculation).

### § 3. Gravioptic effects of General Relativity

Let us observe these traditional effects from the point of view of Newton's mechanics, which, by the way, can explain all the effects of General Relativity by itself. We expect to find out something, which has escaped relativists' attention.

We use the principle of mass and energy equivalence of A. Einstein's General Relativity, which was proposed by Hevyside, i.e.

$$m = \frac{hv}{c^2}. \quad (187)$$

Since, evidently, all masses are equivalent for the gravitation field then that belongs to a photon as well. In the gravitation field the photon must change its trajectory or its energy or the both parameters at the same time. Let us view limit cases of this motion.

a) The photon vertical failure in the gravitation field

In the case of the photon vertical failure with  $g$  acceleration in the gravitation field it obtains an additional energy:

$$\Delta E = m \cdot g \cdot \Delta l, \quad (188)$$

where  $l$  is the traversed path.

Since the light speed is a constant then the photon can change its energy by the only way of changing its frequency:

$$\Delta E = h\Delta\nu = m \cdot g \cdot \Delta l. \quad (189)$$

Taking the relation of

$$\frac{\Delta E}{E} = \frac{h\Delta\nu}{h\nu} = \frac{m \cdot g \cdot \Delta l}{mc^2} = \frac{g \cdot \Delta l}{c^2} \quad (190)$$

we derive

$$\pm \frac{\Delta\nu}{\nu} = \frac{g \cdot \Delta l}{c^2} = \frac{\Delta l}{c^2} \text{ grad } \varphi = \frac{\Delta\varphi}{c^2}, \quad (191)$$

i.e. the classical equation of GR, where  $g = \text{grad } \varphi$ .

The sign of  $\pm$  means that the photon can accelerate or decelerate depending on the direction of motion relatively the gravity field, i.e. the frequency displacement can be “red” or “blue”. Since the photon is a neutral particle then an artificial non-homogeneous gravitation field is a finished accelerator of neutral elementary particles!

b) The curvature of the optic beam, which moves parallel to a gravitating surface

The case is that in the gravity field the photon traverses the path of  $\Delta l$  parallel to the gravitating surface. At the motion it obtains a vertical component of speed of

$$V_{\perp} = g \cdot \Delta t = g \frac{\Delta l}{c}. \quad (192)$$

Hence, trajectory curvature for small angles is

$$\Theta = \frac{V_{\perp}}{c} = \frac{g \cdot \Delta l}{c^2} = \frac{\Delta l}{c^2} \text{grad } \varphi = \frac{\Delta \varphi}{c^2}, \quad (193)$$

i.e. we obtain the result of GR, which is accurate to the multiplier of 4. Since we are interested in not cosmic effects but in laboratory ones we use our equations. Draw attention to the fact that both the frequency displacement and the trajectory curvature are described by the same equation in spite of the fact that one effect is longitudinal and the second one is transversal relatively the gravity acceleration. One more detail is any effect verges towards zero in the path of  $\Delta l \rightarrow 0$ . We will use it discussing experimental results... Substituting  $\text{grad } \varphi$  in the equations (191, 193) by the equation (170) we derive the equation of gravioptic effects, which occur in the non-homogeneously magnetized ferromagnetic:

$$\pm \frac{\Delta v}{v} = \Theta = \frac{1.4 \cdot 10^{-5} \cdot l}{(BH)_s} \text{grad}(BH). \quad (194)$$

c) Square gravioptic effect

This effect has not ever been observed by anyone. Let us return to the photon trajectory curvature. Making horizontal motion by the path of  $\Delta l$  it simultaneously makes vertical motion by the path of  $\Delta h$ :

$$\Delta h = g \frac{\Delta t^2}{2} = \frac{g}{2} \left( \frac{\Delta l}{c} \right)^2, \quad (195)$$

i.e. it again obtains the additional energy of

$$\Delta E = m \cdot g \cdot \Delta h \quad (196)$$

in spite of the fact that in this case it falls “sideways”. However, that does not change anything. Hence as well as it occurs in the case of vertical motion the photon must increase its frequency on the value of

$$+ \frac{\Delta v}{v} = \frac{\Delta h \cdot g}{c^2} = \frac{1}{2} \left( \frac{\Delta l \cdot g}{c^2} \right)^2 = \frac{1}{2} \left( \frac{\Delta l}{c^2} \text{grad } \varphi \right)^2 = \frac{1}{2} \left( \frac{\Delta \varphi}{c^2} \right)^2. \quad (197)$$

This effect is quite visible in laboratory conditions, and the frequency displacement of optic radiation can come to hundreds of kilohertz. For a ferromagnetic this equation becomes

$$\frac{\Delta\nu}{\nu} = \frac{1}{2} \left[ \frac{l \cdot 1.4 \cdot 10^{-5}}{(BH)_s} grad(BH) \right]. \quad (198)$$

#### § 4. Frequency gravitational displacement of the optic radiation occurring in the non-homogeneously ferromagnetic

Observability of this effect was predicted by the author in 1976 [21]. The effect was investigated in 1978-1980 and published in 1983 [22]. As it has been demonstrated in the previous paragraph in a non-homogeneously magnetized ferromagnetic both the gravioptic effects of GR are described by the same equation:

$$\pm \frac{\Delta\nu}{\nu} = \Theta = \frac{1.4 \cdot 10^{-5} \cdot l}{(BH)_s} grad_z(BH). \quad (194)$$

The dependence of  $grad_z(BH) = f(H)$ , which has been calculated due to the results of magnetic calculations, is represented in Fig.66.

As it can be seen from Fig.68 qualitative coincidence of the theoretical results with experimental ones does not raise doubts. Their certain quantitative difference can be explained by the fact that the magnetic and optic measurements were made with the different material. It should be noted that interferometric measurements were made in a permanent magnet and heterodyne measurements were made in an electromagnet. The frequency displacement is a value of  $10^{-5}$  order, and since the gravitational curvature of light is described by the same equation, i.e. a value of the same order (difference contains the length of the working dishes, i.e.  $l$  parameter) then, hence, the very gravitational part of the curvature effect was unobservable in 1975!

Experiment  
Interferometer

Experiment  
Oscillator

Calculation

Fig.68

Dependence of  $\frac{\Delta\nu}{\nu} = f(H)$ . Calculation and experiment.

This experiment was remade by two students of Moscow Physical Technical Institute in 1983 (the author was a tutor).

## § 5. Square gravioptic effect

As it has been mentioned above the essence of the effect lies in the fact that the beam curvature in the non-homogeneously magnetized ferromagnetic must be accompanied by the frequency displacement of the optic beam at the output of the working medium, which is described by the equation of

$$\frac{\Delta\nu}{\nu} = + \frac{1}{2} \left[ l \cdot 1.4 \cdot 10^{-5} \frac{\text{grad}(BH)}{(BH)_s} \right]^2. \quad (198)$$

In light of that an immediate experimental testing is impossible we have to use only the theoretical dependence of  $\frac{\Delta\nu}{\nu} = f(H)$ , which has been calculated due to the real parameters of the solution of  $MnCl_2$  and is demonstrated in Fig.69.

Fig.69  
“Square” gravioptic effect (calculation).

Apart from practical value (this effect is necessary to be taken into account designing optic communication systems, in which ferromagnetic switchboards are used) this effect can cause possible disclosure of asymmetry of Maxwell’s system of equations relatively the gravitation field and the gravitation energy.

Actually real, physically valid connection of magnetism with gravitation is derived from the electron microstructural model, which has appeared to be correct. The connection of electrostatic with gravitation does not follow anything.

The light beam curvature, which occurs in the non-homogeneously magnetized ferromagnetic, should be accompanied by observable displacement of the beam frequency. However, we can curve the beam in a “non-homogeneously electrified” optically transparent ferroelectric...

Is it accompanied by the displacement of the beam frequency?

Only an experiment can answer. The asymmetry of Maxwell’s equations relatively the gravitation should appear here.

## § 6. Some fantastic opportunities opening up before the modern fundamental science

The proved regular connection of magnetism with gravity opens up new opportunities to solve limit tasks of the fundamental science.

- a) Gravimagnetic neutrino trap

Intensive work at neutrino detecting is doing all other the world. The particular interest to this problem is caused by the fact that it is the only kind of radiation, which comes to us undistorted from solar and

stellar depths, i.e. it contains true information of occurring processes. However, huge penetrability (at the energy of 1 MeV free path in lead is equal to  $10^{20}$ , i.e. 100 light years) produces serious difficulties in the experimental work. Actually modern neutrino detectors fix less than 1 event (capture) per a minute at the flow density of reactor anti-neutrinos of  $10^{13} \text{ cm}^{-2}$  order. That is explained by extreme infinitesimal of the capture cross-section, which comes to about  $10^{-43} \text{ cm}^{-2}$ . Our proposal is following. If the same neutrino is made to interact with the same detector  $10^{10}$  times instead of 1 time as it has a place in modern apparatus, then this value can be  $10^{10}$  times increased.

How can it be realized?

From our point of view, which is expected not to conflict with fundamental science, all masses are equal in the face of gravitation. In this view the trajectory curvature of the neutral photon is equal to the trajectory curvature of the neutral neutrino, as parameters of the very particle are not included into the equation of the effect. If it is so then a closed ring of the non-homogeneously magnetized ferromagnetic is an ideal trap for any neutrino and any energy because any ferromagnetic is identical to vacuum with relation to neutrino penetrability.

Let us evaluate the radius of the curvature of the neutrino trap according to the results of our gravioptic experiments. The effect of the frequency displacement came to  $10^{-5}$  order that is equal to the effect of the gravitation curvature of the light beam, which is evaluated in radians. Accepting this value as the curvature we immediately derive the radius of the trap:

$$R = 10^5 \text{ cm} = 1 \text{ km}. \quad (199)$$

Thus we have made sure that the neutrino trap is of rational size, which can be decreased by using of strong ferromagnetics. Surely, in this case a lot of difficulties will become apparent, which, for example, are connected with adjustment etc. In this connection the main thing is that for the neutrino the trap is a full equivalent of a controlled “black hole”.

Thus there is one more fundamental application for our amateur’s experiments.

#### b) Solar neutrino detector

As it is known, in general solar neutrinos are electronic. A reaction of nuclear capture is the basic mechanism of detecting for them:



The energy threshold of the reaction is equal to 0.814 MeV whereas the main flow of the solar neutrinos consists of corpuscles of energy of 0.42 MeV. Chlorine is absolutely insensitive to them. Finally the rate of  $\text{Ar}^{37}$  generation does not exceeds 0.3 – 0.4 of atom per a day [23]. A solution of the case may lie in the neutrino acceleration to duplication of its energy.

As it has been mentioned above the frequency displacement can be “red” as well as “blue” depending on the direction of the particle motion relatively the gradient of the scalar gravitation potential (the gravity acceleration).

Let us calculate the track length of the particle, which is necessary to double its energy.

$$\frac{\Delta E}{mc^2} = \frac{\Delta m}{m} = \frac{g \cdot \Delta l}{c^2} = 1 \quad (201)$$

at  $g_{\text{exp}} = 4.6 \cdot 10^{15} \text{ cm/sec}^2$ ,  $\Delta l \cong 1.95 \text{ km}$ .

At a full length of accelerating part of 100 meters it requires 20 neutrino turns in the gravitation trap to start proceeding of the reaction of neutrino capture by the chlorine atom. If the trap radius is about 1 km then 100 m is just 1.6% of the general length of the gravitation ring. It may be expected that in the case of uniform placing of “accelerating” elements in the space among “curving” elements the condition of the closing of the flow is not broken. Using of the manganese chloride (by the way, its crystal phase can be used as well) as an accelerator is favourable because the reaction of capture occurs in it.

Moreover, this method is interesting for the fact that it is possible to create accelerating cells, which take into account the neutrino sperality. In our opinion, to achieve this aim it is enough to coincide the direction of the scalar gravitation potential with the direction of the impressed magnetic field.

It s evident that change of the magnetic field sign does not change the sign of the gradient of the scalar potential but it can change the effectiveness of the mechanism of nuclear capture of the neutrino.

We hope that our proposals will attract interest of those physicists who deal with the problem of neutrino. It seems that this way can lead not only to more effective results of investigations but to significant saving of costs for measuring apparatus development, which amount to millions.

## § 7. Short gravitation impulses generator

Work on the gravitation impulses is divided into two stages.

1. The stage of proving, where it is necessary to radiate and to detect the gravitation radiation impulse and to clearly prove that neither electromagnetism nor acoustics concern the observing impulse.
2. The stage of introduction, which require wide previous investigations of peculiarities of the new canal of information transmission. It requires rough evaluation of the propagation constants. It is necessary to estimate conditions of the most optimal operation of the constituents of the communication canals, ways of increase of the radiation directedness and many other parameters.

Absolutely different demands are made of these two stages. The first stage requires minimal appearance of electromagnetic accompany of the gravitation radiation impulse, the duration is unimportant (the power has to be enough). The second stage requires certain duration of the radiation impulse.

The first case is easy to be realized by mechanical means, which have been described in the previous parts of the work. However their impulse duration limit lies approximately in the area of  $10^{-2}$  sec. Really we just have the impulse of about 0.5 sec. Nevertheless it is necessary to have a real prospect of compacting of the information canal to serious work on creation of communication systems operating on gravitation waves. Above all the compacting should be done due to shortening of the gravitation radiation impulse.

In this connection the proved regularity of the connection of the magnetism with the gravitation shows the only way to solve the problem, i.e. the creation of ferromagnetic impulse generators of the gravitation radiation. Actually, the equation, which connects the magnetic energy with the gravitation one (87), of

$$W = \frac{BHV}{\alpha} = \frac{\mu H^2 V}{\alpha} = \frac{B^2 V}{\mu \alpha}$$

is easily followed by the equation of the gravitation radiation power, i.e.

$$W = \frac{2BV}{\mu\alpha} \frac{dB}{dt} = \frac{B^2 V}{\mu^2 \alpha} \frac{d\mu}{dt}. \quad (202)$$

Thus, even a usual technical remagnetization is accompanied by the gravitation radiation.

To prove this fact it is necessary to use a receiver of just gravitation impulses with a working stripe, which ensures the reliability of the receiving. Unfortunately, we have not succeeded in it. Nevertheless a laboratory model the generator of the gravitation impulses of about 1-microsecond duration (due to a feed circuit) and of 100-kWt/imp power (due to the feed circuit as well) has already been created by us.

The general view of the generator is demonstrated in Fig.70, where the very radiator (1) is fixed on a system of controlled rods (2) and is fed by a source of powerful electromagnetic impulses, which are located in a body (3), which at the same time is a support of a system of space scanning of the gravitation ray. The scanning limits are  $360^\circ$  by azimuth, and  $\pm 30^\circ$  by vertical. The device is supplied with a remote-control console (4), which provides with possibility to work in tephraph mode.

Fig.70  
Impulse generator

The general mass of the generator is about 40 kg, the mass of the radiator is about 25 kg. The radiator is Lobachevsky's pseudosphere made of a superparamagnetic, which mass is equal to 6 kg. It is placed into a magnetic bias field generated by permanent magnets. The pseudosphere is biased by an outer current impulse, which is applied to a special winding. The pseudosphere is placed inside it. The device is fed by electric energy source of 50 Hz, 220 V.

Unfortunately, all that we know about it is that it operates and its radiation warms a hand.

To indicate the very gravitation component it is necessary to use a receiver with a stripe of 10 MHz, which is inaccessible by now. Nevertheless a powerful generator of microsecond impulses, which is quite good for the first experiments, already exists. To increase power up to 1 megawatt at the input of the radiator is not a problem for us. The spade-work has already been done.

## § 8. The problem of gravitation source

On our mind gravitational antennas and gravitational receivers of Weber's type, on which the fundamental science is oriented, are nonsense. Surely, it is senseless to absolutely deny the fact of principle possibility to indicate mechanical auto-oscillations of a 1.5 – 3-ton massive metal blank. The technics of nowadays level can do much more significant things. However, from our point of view, it seems more senseless the very fact of “expecting” of density waves auto-excitation in a trial mass under the action of an unscreenable and all-penetrating radiation (of a local source, which is undefined in the space). The direction of the radiation should coincide by chance with the axis of a trial body.

We handle the problem of the receiver from other positions.

1. The gravitation radiation must interact with the gravitation field of a rotating mass instead of the mass penetrated by the radiation without losses (all-penetrating). The interaction with the gravitation field of the rotating mass must be the most effective because of a principle of physical processes reciprocity.
2. A gravitational detector as a directly measured value must use the angular speed of free rotation of a thin disk of a great diameter instead of the density waves of the massive blank.

From our equation of gravitation energy of a rotating body (97) of

$$W = 2k\gamma_0\omega^{3/2} \frac{m^2}{r}$$

we can easily derive an equation for the angular speed increment of the rotating body under the action of the gravitation radiation impulse, i.e.

$$\pm \Delta\omega = \frac{90r}{\omega^{1/2}m^2} \cdot \alpha \cdot \Delta W$$

at  $k=0.5$ ,

where  $\Delta\omega$  is an impulse of change of rotation frequency of the trial mass (of the disk)

$r$  is the radius of the disk,

$m$  is the mass of the disk,

$\Delta W$  is the energy of the gravitation radiation impulse,

$\alpha$  is a parameter of gravitation power loss in the detector.

It is evident that our equation requires the mass to be as small as possible, and the radius to be as big as possible.

As for  $\omega$  rotation frequency, the issue remains open because  $\alpha$  parameter of loss is supposed to be a function of the frequency. In general, we have an opportunity to experimentally prove it. Thus detecting the gravitation impulse we measure not casual auto-oscillations of the blank but regular changes of rotation frequency of the light disk. Therefore our apparatus do not weigh tons. Together with autonomic feed sources it weights kilograms.

Three basic types of indication of  $\Delta\omega$  may be used here:

1. a usual tachometer generator,
2. an analogy transformer of frequency into amplitude,
3. a numerical transformer of frequency into amplitude.

Now we will not touch the peculiarities of the detector construction and of electric schemes because this material is for another work. We just can declare with certainty that the next model of the receiver will have the stripe of about 10 MHz, and the third generation of the models will have the stripe of about 5 GHz. To solve these problems it requires nothing but the devices, which has already been producing by nowadays industry.

## Conclusion

A repeated testing of a mechanism of connection of the magnetism with the gravitation, which has been observed in this book, demonstrated the following facts.

1. Supposing the phenomenon of the magnetostriction to be a matter compression in its proper gravitation field we made several experiments and calculations. They include numerical calculation of magnetostriction curves, taking curves of technical magnetization, and comparison of the calculation results with the known experimental results of magnetostriction. The results have proved our supposition!

The most interesting fact is that the gravitation has been placed into the equation as the constant of the magnetostriction, which appeared to be equal to the gravitation energy of a ferromagnetic in the point of magnetization saturation.

2. The effect of magnetostriction curvature of an optic beam in a non-homogeneously magnetized ferromagnetic, which was predicted and discovered by the author in 1975, can be considered as a proved fact.
3. The effect of displacement of optic radiation frequency in a non-homogeneously magnetized ferromagnetic can be considered as finally explained (it was predicted by the author in 1976, and investigated in 1980).
4. Light beam curvature in a non-homogeneously magnetized ferromagnetic must be accompanied by its frequency displacement, according to the square law in this case. This effect is very interesting from the point of theory since it allow experimentally state whether Maxwell's equations are symmetrical relatively the gravitation or not.
5. It is possible to design a gravitational neutrino trap, hence, to create a neutrino detector of a new type, which effectiveness can be ten orders higher than the effectiveness of nowadays neutrino detectors.
6. It is possible to create short-impulse and high-speed generators of gravitation impulses of great power.
7. The problem of the gravitational detector (receiver) has a new solution, which principally differs from the methods applied in the world modern science.
8. The electron model proposed by the author has been experimentally proved as all the theory predictions, which are the consequence from the model, have been confirmed.
9. According to provisional data the propagation speed of the gravitation radiation impulses for a "dipole" oscillator lies in the interval of  $(3 \cdot 10^8 - 3 \cdot 10^9) \cdot c$ , and for a quadrupole radiation it is equal exactly to  $3 \cdot 10^{10} c$ . Obviously, The value of  $3 \cdot 10^{10} c$  is the second constant of matter propagation in the Nature.
10. the task of gravitation power propagation is a problem of non-linear mechanics. Probably, D'Alamber was the first to realize it. He raised the question of "motion of a material point in a four-dimensional space". Nobody has succeeded in making final analytical results of this problem.

The authors hope that the material stated above will awake interest of wide circle of people concerned with modern Science. Good luck!

## References

1. Иваненко Д.Д., Пронин П.И., Сарданашвили Г.А. Калибровочная теория гравитации. М.: Изд. МГУ, 1985. С. 113.
2. Сверхкороткие оптические импульсы / под ред. Шапиро. М.: Мир, 1981. С.68, 83.
3. Макс Борн. Атомная физика. М.: Мир, 1970. С.444
4. Тамм И.Е. Основы теории электричества. М.: ГИТТЛ, 1957. С. 97
5. Горелик Г.С. Колебания и волны. Гл. VII. М.: Наука, 1959.
6. Белов К.П. Магнитные превращения. М. 1959. С. 111 – 115.
7. David R. Mikkelsen and Michael J. Newmann. Constraints on the gravitation constant at large distances. // Phys. Rev. D. 1977. Vol. 16, No 4. P. 919 – 926.
8. Hsou-Taou Yu and Vei-Tou Ni. Experimental determination of the gravitational forces at separation around 10 meters. // Phys. Rev. D. 1979. Vol. 20, No 8. P. 1813 – 1815.
9. Шарлье К. Небесная механика. М.: Наука, 1966.
10. Лаплас П.С. Изложение системы мира. Л.: Наука, кн. 4. – 198. С. 197 (see also Лаплас П.С. Изложение системы мира. 1961. СПб, т. 1. С. 418; т. 2. – С. 412).
11. Киренский Л. В. Магнетизм. М., Наука, 1967. С. 94 – 107.
12. Ацюковский В.А. Введение в эфиродинамику. Деп. ВИНТИ № 2/60-80. Удк 530.3. М., 1980. С. 219.
13. Гильзин К.А. Электрические межпланетные корабли. М.: Наука, 1970.
14. Robert L. Forward. General Relativity for the Experimentalist. Proc. IRE. 1961. Vol. 49. P. 892 – 912.
15. Edward Teller. Electromagnetism and Gravitation. // Proc. Nat. Acad. Sci. USA. Vol. 74, No 4. P. 2664 – 2666.
16. Physical Encyclopedia. Moscow., 1963. Vol. 3, P. 109.
17. Вонсовский С.В. Магнетизм. М.: Наука, 1971. С. 404.
18. Фриш С.Э., Тиморева А.В. Курс физики. Т. 3. М., 1952. С. 251.
19. Поляков С.М., Мартынов В.Ф. Способ отклонения и фокусирования оптического излучения. – Patent claim №2187534/25 of 10.11.1975.
20. Катыс Г.П., Кравцов Н.В., Чирков Л.Е., Коновалов С.М. Модуляция и отклонение оптического излучения. М.: Наука, 1967. С.141.
21. Поляков С.М. Способ управления частотой оптического излучения. – Patent claim № 2324523/25 of 13.02.1976.
22. Поляков С.М., Олихов И.М., Дорофеев В.А., Ладанов Г.И. Каневский Е.И. Смещение частоты оптического излучения в неоднородно намагниченном ферромагнетике // Изв. АН МССР. Сер. Физико-технических и математических наук. 1983. № 2. С. 57 – 59.
23. Физика микромира. М.: Советская энциклопедия, 1980. С. 274 – 281.
24. Дубровский В.А. Упругая модель физического вакуума. ДАН СССР. Т. 282, №1. С. 83 – 88.

## Contents

Introduction into Experimental Gravitonics .....	1
Part I	
Research for Ways of Solution of the Problem of Powerful Laboratory Sources of Gravitation radiation .....	3
Chapter 1	
New notions of long ago forgotten concepts .....	3
§ 1. Is the “light barrier” penetrable? .....	3
§ 2. Energy proportions and mechanism of “c-barrier” establishing .....	5
§3. How much is a photon “electric length”, and how many lengths are contained in one quantum of electromagnetic radiation? .....	9
§4. Is photon a one-massed or two-massed particle? .....	10
Chapter 2	
Photon and electron microstructural model .....	12
§ 1. What do we know of a photon as a quantum of electromagnetic energy? .....	13
§ 2. Uniquantum parameters .....	14
§ 3. Photon model .....	21
§ 4. Electron phenomenological microstructural model .....	22
§5. Derivation of approximate gravitational equations, which have practical value .....	29
Part II	
Experimental Testing of New Gravitational Equations .....	37
Chapter 1	
Experimental testing of mechanical gravitational equations .....	37
§ 1. Problems of speed of gravitation radiation propagation .....	37
§ 2. Method of measuring of the speed of an unknown radiation propagation according to the recoil momentum. ....	38
§ 3. An experimental device description .....	41
§ 4. A gyroscope multipole of “Bouquet” .....	44
§ 5. Investigation of the effects of impact rotation of the massive gyroscope .....	49
§ 6. The effect of impact break of the massive rotating gyroscope. ....	50
§ 7. A quadrupole generator of directed gravitation radiation (“Yolka” (“Fir-tree”)) .....	51
§ 8. Experimental results for the quadrupole generator .....	55
§ 9. A mathematical model of the quadrupole generator .....	57
§ 10. The issues of practical application of the obtained results .....	67
Chapter 2	
Experimental Proof of Regularity of Connection of Magnetism with Gravitation as Consequence of Electron Microstructural model .....	69
§ 1. Gravitational interpretation of a magnetostriction .....	71
§ 2. Magnetostriction curvature of an optic beam .....	74
§ 3. Gravioptic effects of General Relativity .....	79
§ 4. Frequency gravitational displacement of the optic radiation occurring in the non-homogeneously ferromagnetic .....	81
§ 5. Square gravioptic effect .....	82
§ 6. Some fantastic opportunities opening up before the modern fundamental science .....	82
§ 7. Short gravitation impulses generator .....	84
§ 8. The problem of gravitation source .....	86
Conclusion .....	87
References .....	88